

Design, Rapid Prototyping and Testing of the Wells Turbine

by

Megat Fazli bin Rozli

Dissertation submitted in partial fulfilment of
the requirements for the
Bachelor of Engineering (Hons)
(Mechanical Engineering)

JANUARY 2009

**Universiti Teknologi PETRONAS
Bandar Seri Iskandar
31750 Tronoh
Perak Darul Ridzuan**

CERTIFICATION OF APPROVAL

Design, Rapid Prototyping and Testing of the Wells Turbine

by

Megat Fazli bin Rozli

A project dissertation submitted to the
Mechanical Engineering Programme
Universiti Teknologi PETRONAS
in partial fulfilment of the requirement for the
BACHELOR OF ENGINEERING (Hons)
(MECHANICAL ENGINEERING)

Approved by,



(DR. AZMI ABDUL WAHAB)

Dr. Azmi Abd Wahab
Lecturer
Mechanical Engineering Department
Universiti Teknologi PETRONAS
Bandar Seri Iskandar, 31750 Tronoh
Perak Darul Ridzuan, Malaysia.

UNIVERSITI TEKNOLOGI PETRONAS

TRONOH, PERAK

January 2009

CERTIFICATION OF ORIGINALITY

This is to certify that I am responsible for the work submitted in this project, that the original work is my own except as specified in the references and acknowledgements, and that the original work contained herein have not been undertaken or done by unspecified sources or persons.


MEGAT FAZLI BIN ROZLI

ABSTRACT

This project is to design, manufacture and testing the Wells turbine. In order to know the performance of the Wells turbine, a prototype is developed. Computer Aided Three Dimensional Interactive Application (CATIA) is used in the 3D solid modelling design for Wells turbine prototype components. Design is carried out to suit the testing requirements. A scale model is designed based on the actual dimension of Wells turbine. Study is focus on the variations and manipulations of the testing parameters of Wind Tunnel on the designed rotor and the effect on the rotation of the rotor as well as on the workability of the material used to fabricate the rotor. Rapid Prototyping (RP) machine is used to manufacture the rotor by using the 3D solid modelling data from CATIA. Rapid Prototyping process will shorter the manufacturing time before testing. Rapid Prototyping process has the limitation; therefore, the 3D solid model design must be suitable with the machining capability. Wind Tunnel is used to test the Wells turbine prototype with different parameter settings. Testing is carried out on the prototype to determine the minimum velocity of air that will rotates the rotor and the maximum rotational speed in revolution per minute (rpm) of the rotor.

ACKNOWLEDGEMENTS

The author wishes to take the opportunity to express his utmost gratitude to the individual that have taken the time and effort to help the author in completing the project. Without the cooperation of these individuals, no doubt the author would have faced some minor complications through out the course.

First the author's utmost gratitude goes to the author's supervisor, Dr. Azmi Abdul Wahab. Without his guidance, advices and patience, the author would not be succeeded to complete the project. To the Final Year Research Project Coordinator, Prof. Vijay and Dr. Puteri Sri Melor for provide him with all the initial information required to begin the project.

To the entire technician in Mechanical Engineering Department, thank you for helping the author in completing her project.

To all individuals that has helped the author in any way, but whose name is not mentioned here, the author thanks you all.

TABLE OF CONTENTS

| | | |
|-------------------------------------|--|-----|
| CERTIFICATION OF APPROVAL | | i |
| CERTIFICATION OF ORIGINALITY | | ii |
| ABSTRACT | | iii |
| ACKNOWLEDGEMENT | | iv |
| CHAPTER 1: | INTRODUCTION | 1 |
| | 1.1 Background | 1 |
| | 1.2 Problem Statement | 1 |
| | 1.3 Objectives | 2 |
| | 1.4 Scope of Study | 2 |
| CHAPTER 2: | LITERATURE REVIEW | 3 |
| | 2.1 Wells Turbine Working Principle | 3 |
| | 2.2 Design of Turbine Blade | 5 |
| | 2.2.1 Design Software | 5 |
| | 2.2.2 National Advisory Committee for Aeronautics (NACA) 4-Digit Airfoil Design | 5 |
| | 2.3 Fabrication | 7 |
| | 2.3.1 Rapid Prototyping | 7 |
| | 2.4 Laboratory Tests | 8 |
| CHAPTER 3: | METHODOLOGY | 11 |
| | 3.1 Literature Review | 12 |
| | 3.2 Prototype Wells Turbine Design | 12 |
| | 3.2.1 Conceptual Design of 3D Solid Modelling of Wells Turbine Prototype | 12 |
| | 3.2.2 Conceptual Design Analysis of Wells Turbine Prototype | 13 |
| | 3.2.3 Bearing Selection | 17 |
| | 3.2.4 Turbine Blade and Rotor Design | 20 |
| | 3.2.5 3D Solid Modelling of the Conceptual Design of Wells Turbine Prototype | 21 |
| | 3.3 Prototype Wells Turbine Prototyping and Fabrication | 22 |
| | 3.3.1 Multi Jet Modeling (MJM) Machine Working Principle | 22 |
| | 3.3.2 Material Use in Multi Jet Modeling (MJM) | 24 |
| | 3.3.3 Rotor-shaft by Rapid Prototyping (RP) Process | 24 |
| | 3.3.4 Manufacturing Processes of Support Structure | 25 |

| | | | |
|-------------------|---|-------|----|
| 3.3.5 | Parts Assembly Process | . . . | 28 |
| 3.4 | Prototype Wells Turbine Testing | . . . | 30 |
| 3.5 | Analysis on the Results and Findings. | . . . | 31 |
| CHAPTER 4: | RESULT AND DISCUSSION. | . . . | 32 |
| 4.1 | Testing Failure for First Configuration | . . . | 32 |
| 4.2 | Design of Second Configuration | . . . | 33 |
| 4.3 | 3D Solid Modelling Design by CATIA | . . . | 36 |
| 4.4 | Blade Design Modification | . . . | 37 |
| 4.5 | Result Analysis | . . . | 38 |
| CHAPTER 5: | CONCLUSION AND RECOMMENDATION | . . . | 42 |
| REFERENCES | | . . . | 44 |
| APPENDICES | | . . . | 45 |

LIST OF FIGURES

| | | |
|------------|---|----|
| Figure 1: | OWC Device | 3 |
| Figure 2: | Symmetrical turbine blade | 4 |
| Figure 3: | Characteristic of the NACA 4-digit airfoil | 6 |
| Figure 4: | Rapid Prototyping (RP) slicing | 7 |
| Figure 5: | Flow Process of the project | 11 |
| Figure 6: | 3D Conceptual design | 13 |
| Figure 7: | Prototype 2D Structure | 13 |
| Figure 8: | Rotor-shaft 2D Structure | 14 |
| Figure 9: | Rotor-shaft Centroid Analysis | 14 |
| Figure 10: | Centroid of rotor-shaft part | 15 |
| Figure 11: | Coplanar Force System of Rotor-shaft Structure | 16 |
| Figure 12: | Coplanar Force Magnitude and Direction on Rotor-shaft Structure | 17 |
| Figure 13: | Deep Groove Ball Bearing | 18 |
| Figure 14: | NACA 0020 Profile | 20 |
| Figure 15: | Assembly Drawing of Prototype Parts | 22 |
| Figure 16: | Multi Jet Modelling (MJM) | 23 |
| Figure 17: | After Rapid Prototyping (RP) Process | 24 |
| Figure 18: | Material preparation | 25 |
| Figure 19: | Linear Hack Saw Machine | 26 |
| Figure 20: | Squaring process using Conventional Milling Machine | 27 |
| Figure 21: | Boring of Bearing Mounting by CNC Milling | 28 |
| Figure 22: | 2-Dimensional Assembly Drawing | 29 |
| Figure 23: | Wells Turbine Prototype | 30 |
| Figure 24: | Blade of first configuration | 32 |
| Figure 25: | Rotor-shaft 2D part | 33 |
| Figure 26: | Rotor-shaft Centroid Analysis | 33 |
| Figure 27: | Centroid of Rotor-shaft Part | 34 |
| Figure 28: | Coplanar Force System of Rotor-shaft Part | 35 |
| Figure 29: | Coplanar Force Magnitude and Direction on Rotor-shaft Part | 36 |
| Figure 30: | Assembly Drawing of Prototype Parts | 36 |
| Figure 31: | Blade of new configuration | 37 |
| Figure 32: | NACA 0020, Lift Coefficient, C_L and Drag Coefficient, C_D vs α | 38 |
| Figure 33: | NACA 0020, Lift Force, F_L and Drag Force, F_D vs Air Velocity | 39 |
| Figure 34: | Revolution per minute (rpm) vs Air Velocity | 41 |

LIST OF TABLES

| | | |
|----------|---|----|
| Table 1: | Centroid calculation of first configuration of rotor-shaft part | 15 |
| Table 2: | Equivalent Radial Load Factors for Ball Bearings . . . | 45 |
| Table 3: | Dimensions and Load Ratings for Single-Row 02 Series Deep-Groove | 45 |
| Table 4: | Profile of the NACA 0020 | 21 |
| Table 5: | Geometric details of rotor | 21 |
| Table 6: | Centroid calculation of new rotor-shaft part | 34 |
| Table 7: | Profile of the NACA 0020 for new configuration | 37 |

CHAPTER 1

INTRODUCTION

1.1 Background

Wells turbine was invented by Dr. A.A Wells in 1976. It is an alternative method in generating electrical power for useful utilization. It is a pollution-free energy production method compared with the other power generating devices or methods. Wells turbine can be used to convert the kinetic energy of wind into mechanical energy. Then, the mechanical energy can be converted into useful electrical energy. During Wells turbine production, it has to undergo several engineering processes. These processes consist of designing, manufacturing and finally assembly. There are several manufacturing processes involved such as measuring, cutting, machining, rapid prototyping (RP), casting and finishing. The RP can be used to produce the actual geometry of the turbine rotor. Then, the RP part can be used to produce die for casting process. Therefore, longer time was needed to produce Wells turbine.

In this project, the RP rotor was used in the Wells turbine prototype. This prototype was used to evaluate the performance of the Wells turbine in two different geometrical configurations. Further development of the turbine can be performed based on the preliminary evaluations carried out on the RP rotor.

1.2 Problem Statement

The Wells turbine rotates in the same sense regardless of the direction of the air stream. In order to analyze the rotor performance, the minimum velocity required to start the rotation, and the maximum revolution per minute (rpm) it can achieved will need to be determined. Two configurations of this turbine design were required for testing in the wind tunnel. The Wells turbine prototype involves several manufacturing processes such

as cutting, milling, surfacing and squaring which will consumes a lot of time and money to develop it. By using the Rapid Prototyping (RP), time and cost can be reduced to analyze the RP material as a testing specimen by manipulation of the wind tunnel testing parameters.

1.3 Objectives

The objectives of this project are as follows:

- To design two Wells turbine rotors,
- To use the Rapid Prototyping (RP) to fabricate the rotor of the prototypes,
- To test the prototypes in the wind tunnel by manipulation of the testing parameters.

1.4 Scope of study

This project is focused on:

- Study the conceptual design by analyse on the static condition as well as on the mechanical components design of the prototype,
- Design two configurations of rotor and other parts of the prototype,
- Study the Rapid Prototyping (RP) and the type of material used,
- Study the prototype testing in the wind tunnel and the manipulation of the parameters involved that affect the rotor performance,
- Study the results by analyzing the experimental data.

CHAPTER 2

LITERATURE REVIEW

2.1 Wells Turbine Working Principle

The Wells turbine is a low-pressure air turbine developed for use in oscillating-water-column (OWC) wave power plants to avoid the need to rectify the air stream by delicate and expensive valve systems.

Figure 1 shows that, it keeps its sense of rotation in spite of the changing direction of the air stream, which is driven by the rising and falling water surface in a compression chamber. Its blades feature a symmetrical airfoil with its plane of symmetry in the plane of rotation and perpendicular to the air stream.

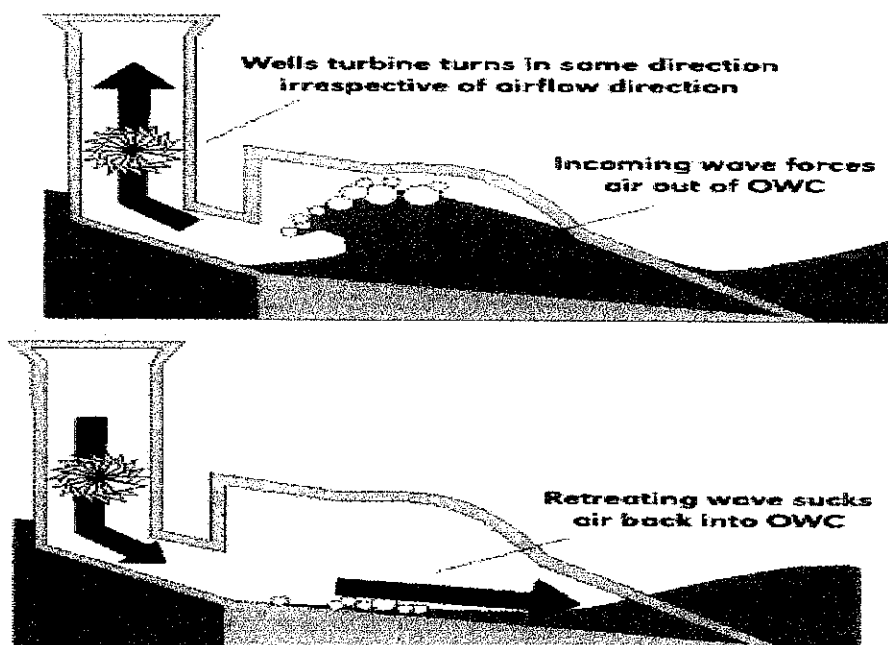


Figure 1: OWC Device

Its efficiency is lower than that of a turbine with constant air stream direction and asymmetric airfoil. One reason is that symmetric airfoils have a higher drag coefficient than asymmetric ones, even under optimal conditions. Also, in the Wells turbine, the symmetric airfoil is used with a high angle of attack (i.e., low blade speed / air speed ratio), as it occurs during air velocity maxima in volatile flow. Then the air stream stalls and lift collapses. The efficiency of the Wells turbine in oscillating flow reaches values between 0.4 and 0.7. (Queen's University Belfast, 1980s).

Wells turbine, invented by A.A Wells, is a self-rectifying airflow turbine. The turbine is capable of converting pneumatic power available in OWC into mechanical energy. It is an axial flow turbine with untwisted rotor blades of symmetrical airfoil section set radially at 90° angle of stagger. Consequently, the turbine rotates in same direction and produces power regardless of which way the air is flowing. Figure 2 below shows the turbine blade is symmetrical with respect to the direction of flow. (NACA, 1915) (M. Govardhan et al., 2007)

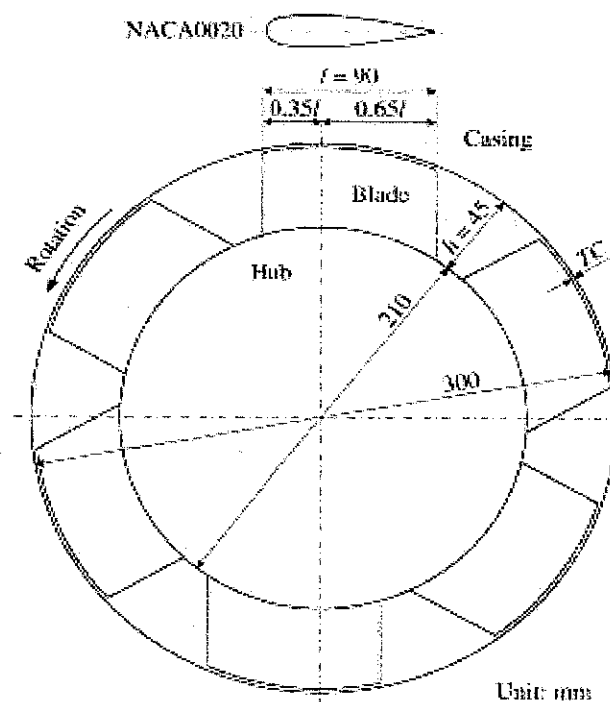


Figure 2: Symmetrical turbine blade

The Wells turbine is a self rectifying air turbine which is expected to be widely used in wave energy devices with the OWC (Ragunathan, 1995). There are many reports which describe the performance of the Wells turbine both at starting and running characteristics. According to these results, however, the Wells turbine has inherent disadvantages in comparison with conventional turbines: lower efficiency and poorer starting characteristics (M. Takao et al., 2006).

2.2 Design of Turbine Blade

2.2.1 Design Software

In the Prototype Wells turbine design, scale model design is made based on the actual dimension of the Wells turbine. Computer Aided Three Dimensional Interactive Application (CATIA) is used to design the 3D solid modeling of the turbine components (Dassault Systemmes, 1981). Various configurations are designed based on the testing requirements. The manipulations variables in design are the number of turbine blades and the shape of the aerofoil which will affect the Wells turbine performance in term of efficiency (Swami Nathan, 1990), (NACA, 1915).

2.2.2 National Advisory Committee for Aeronautics (NACA) 4-Digit Airfoil Design

Although the NACA 4-digit generator function was clearly not created for model blade use, it works rather well. Constrained to produce the symmetrical airfoils used for control line stunters, the generator function is reduced to a simple polynomial equation:

$$y = \pm 0.5(A\sqrt{x} + Bx + Cx^2 + Dx^3 + Ex)^4$$

where y is the vertical coordinate

x is the horizontal coordinate

and the coefficients are $A= 0.2969$, $B= -0.1260$, $C= -0.3516$, $D= 0.2843$, $E= -0.1015$

The output y corresponds to a pair of symmetrical vertical coordinates ($+y$ and $-y$) for a normalized airfoil, whose chord length in x is exactly 1 unit long. The leading edge of the airfoil is located at (x,y) of $(0,0)$, and its trailing edge is at $(1,0)$ (Larry Cunningham; NACA, 1915).

Figure 3 shows the characteristic of the NACA 4-digit airfoil is that its maximum thickness occurs at 30% of the chord length from the leading edge, at $x = 0.3$ on the normalized airfoil. For symmetrical airfoils, the NACA 4-digit airfoils use the numbering **NACA 00nn**, where **nn** is a 2-digit number representing maximum thickness as a percentage of chords. The example airfoil which is 2 inches thick and 10 inches long is a 20% thickness, so its designation would be **NACA 0020** (Larry Cunningham; NACA, 1915).

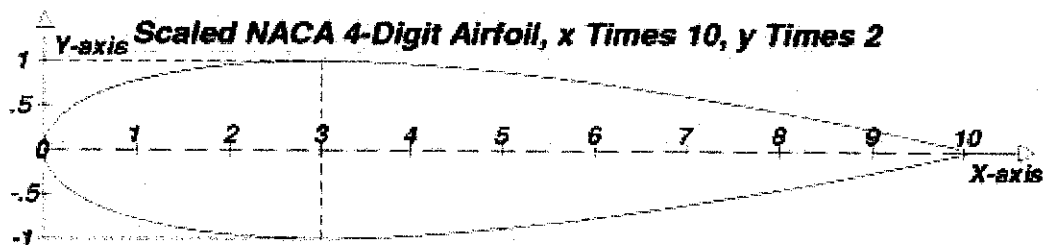


Figure 3: Characteristic of the NACA 4-digit airfoil

To obtain coordinates for a useful airfoil, the normalized airfoil data must be scaled. First, we need to consider the chord (horizontal x length) of the desired airfoil (Larry Cunningham; NACA, 1915).

The blade profile is: **NACA 0020** with chord length of $l= 90$ mm; solidity at mean radius, 0.67; hub-to-tip ratio, 0.7; aspect ratio, 0.5; casing diameter, 300 mm; tip clearance, 0.5 mm; mean radius, $r= 127.5$ mm; width of flow passage $h= 45$ mm. Note

that the adopted turbine rotor is the most promising one in previous studies (Kaneko et al., 1986; Setoguchi et al., 1986).

2.3 Fabrication

2.3.1 Rapid Prototyping

Rapid prototyping (RP) takes virtual designs from computer aided design (CAD) or animation modelling software, transforms them into thin, virtual, horizontal cross-sections and then creates each cross-section in physical space, one after the next until the model is finished. With additive fabrication, the machine reads in data from a CAD drawing and lays down successive layers of liquid, powder, or sheet material, and in this way builds up the model from a series of cross sections. These layers, which correspond to the virtual cross section from the CAD model, are joined together or fused automatically to create the final shape. The primary advantage to additive fabrication is its ability to create almost any shape or geometric feature. Figure 4 shows the rapid prototyping slicing (Grenda E., 2006; Wright, Paul K., 2001; Wohlers, T., 2007).

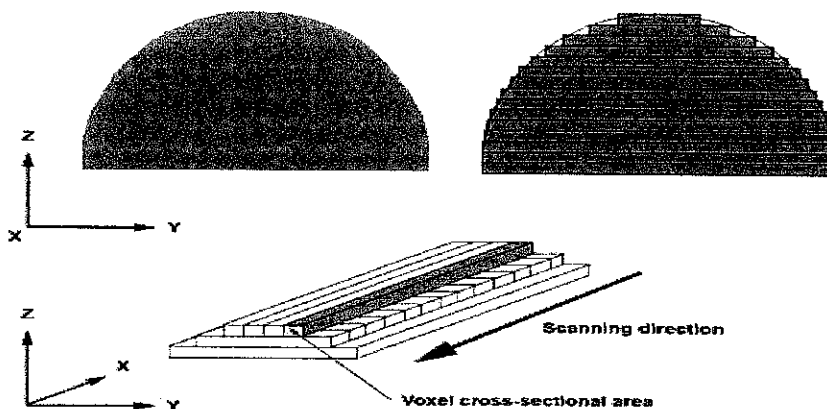


Figure 4: Rapid Prototyping (RP) slicing

The standard data interface between CAD software and the machines is the STL file format. An STL file approximates the shape of a part or assembly using triangular facets. Smaller facets produce a higher quality surface. Some solid freeform fabrication techniques use two materials in the course of constructing parts. The first material is the part material and the second is the support material (to support overhanging features during construction). The support material is later removed by heat or dissolved away with a solvent or water (Grenda, E., 2006; Wright, Paul K., 2001; Wohlers, T., 2007).

The parts produced by rapid prototyping systems are used for several purposes in engineering, including testing of form, fit and function. Form testing allows a designer to verify the CAD design, evaluate manufacturability, and to get reactions from potential users and customers. Fit testing verifies that the designed part mates accurately with adjoining portions of the final assembly. Form and fit testing are also frequently and collectively referred to as "concept modeling". (Castle Island Co.)

Functional testing places the rapid prototyping part in an operating assembly to see if it works. The limited range of rapid prototyping materials has restricted functional testing, but this is improving as higher temperature and more durable materials are introduced for many of the technologies. Objects made by rapid prototyping can also be transferred by means of secondary processes into final materials for testing. (Castle Island Co.)

2.4 Laboratory Tests

Experiments on the RP rotor will be performed using the wind tunnel in Universiti Teknologi PETRONAS (UTP). The prototype is attached to the wind tunnel for performance testing. The overall performance is evaluated by the turbine output torque T_o , the flow rate Q , the total pressure drop across the turbine Δp and the turbine angular velocity, ω (Takao et al., 2007). The flow rate through the turbine Q , whether it is

inhalation (i.e., flow from atmosphere into the settling chamber) or exhalation (i.e., flow from settling chamber to atmosphere) (Kaneko et al., 1986; Setoguchi et al., 1986).

The turbine performance under steady flow conditions is evaluated by turbine efficiency η , torque coefficient C_T and input coefficient C_A against flow coefficient ϕ . The definitions of these parameters areas follow:

$$C_T = \frac{T}{\{\rho(v^2 + U^2)hlzr/2\}}, \quad - (1)$$

$$C_A = \frac{\Delta p T}{\{\rho(v^2 + U^2)hlzr/2\}}, \quad - (2)$$

$$\eta = \frac{T\omega}{\Delta p Q} = \frac{C_T}{(C_A \phi)}, \quad - (3)$$

$$\phi = \frac{v}{U}, \quad - (4)$$

where ρ , v , U and z denote the density of air, axial flow velocity, circumferential velocity at r and number of rotor blades, respectively (Kaneko et al., 1986; Setoguchi et al., 1986).

Besides, the numbers of turbine blade also give a significant in the self-starting mechanism.

Tests were performed with the flow rates up to 0.320 m³/s and the turbine angular velocities up to 471 rad/s. The Reynolds number based on the blade chord was approximately equal to 2.5 x 10⁵. The uncertainty of efficiency is about $\pm 1\%$. This uncertainty is obtained by taking into account the dispersions in the measurement of the physical parameters from which efficiency is obtained (M. Takao et al., 2006).

The performance test of the turbine was carried out by use of newly devised wind tunnel in which it is possible to produce oscillating air flow by controlling the motion of a 1.4 m diameter piston in the cylinder as instructed by a micro-computer (Inoue et al., 1986b;

Setoguchi et al., 1990). In the test of turbine characteristics, the variations of turbine performance with relative inlet angle were examined by changing the rotational speed of rotor so as to cover the effective operating range of the turbine. During the test, the turbine output torque, the air-flow rate and the total pressure drop across the rotor were also measured. The uncertainty of mean efficiency is about ± 2 .

A duct in which the effects of airflow past object can be determined. The steady-state forces on a body held still in moving air are the same as those when the body moves through still air, given the same body shape, speed, and air properties. Scaling laws permit the use of models rather than full-scale objects, such as aircraft or automobiles. Models are less costly and may be modified more easily, and conditions may be simulated in the wind tunnel that would be impossible or dangerous in full scale.

Most data are secured from wind tunnels through measurement of forces and moments, surface pressures, changes produced in the airstream by the model, local temperatures, and motions of dynamically scaled models, and by visual studies.

A balance system separates and measures the six components of the total force. The three forces taken parallel and perpendicular to a flight path are lift, drag, and side force. The three moments about these axes are yawing moment, rolling moment, and pitching moment, respectively.

Surface pressures are measured by connecting orifices flush with the model surface to pressure-measuring devices. Local air load, total surface load, moment about a control surface hinge line, boundary-layer characteristics, and local Mach number may be obtained from pressure data (Cengel, Y.A et al., 2006).

CHAPTER 3

METHODOLOGY

Methods and procedure were established to achieve the objectives of the project. This methods and procedure were relevant and acceptable in completing the project within the given timeframe. The overall flow of the project is shown schematically in Figure 5.

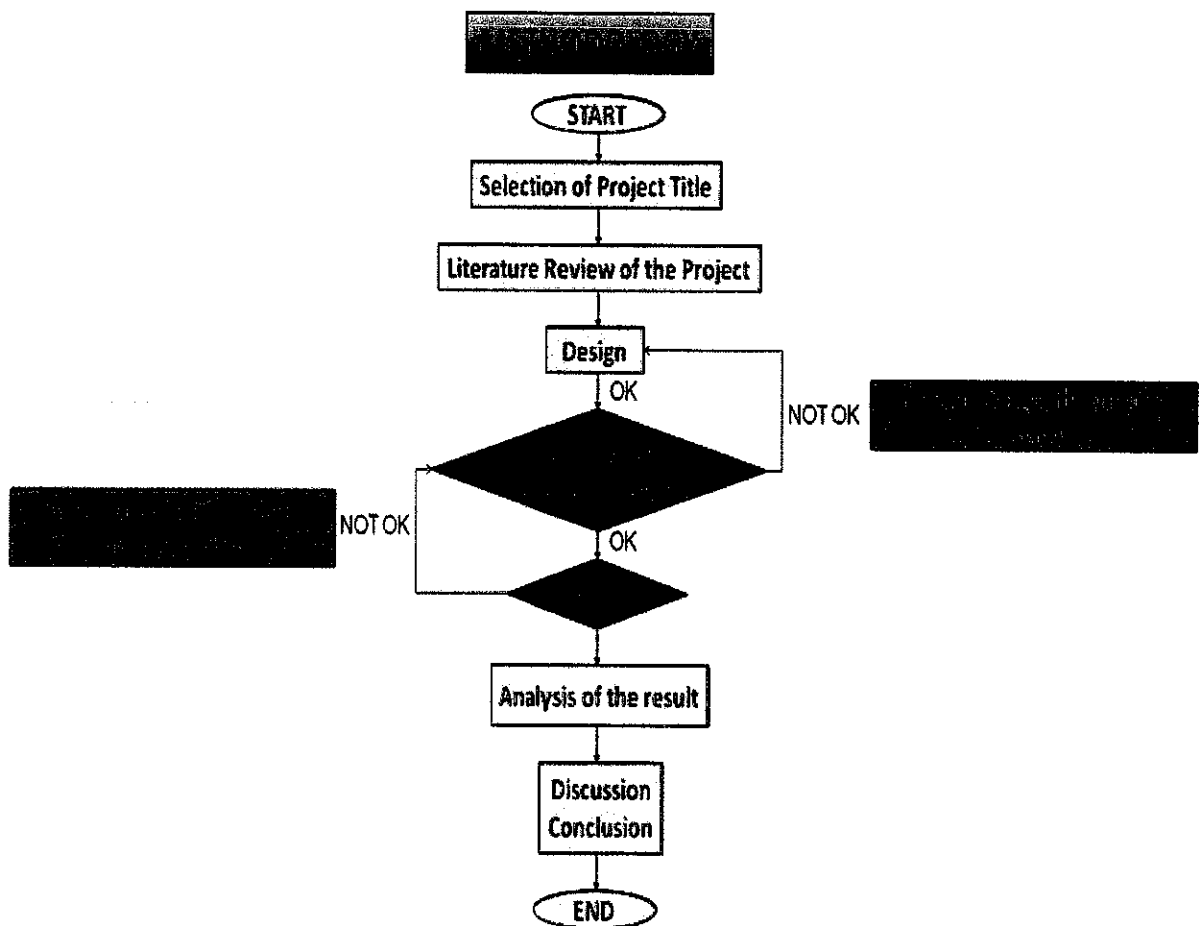


Figure 5: Flow Process of the project

3.1 Literature Review

Literature review were carried out to understand the Wells turbine working principle to complete design of the configuration, fabrication of the parts, testing and evaluation on the results. The literature review was based on the related books, internet and journal paper.

3.2 Prototype Wells Turbine Design

Design process involved conceptual design and 3D solid modelling of parts by using AutoCAD and CATIA software, respectively. Parts were designed to meet the project objectives.

3.2.1 Conceptual Design of 3D Solid Modelling of Wells Turbine Prototype

Figure 6 showed the conceptual design had chosen for the Wells turbine prototype. Design consists of support, hub, blade, shaft and bearing. Conceptual design was developed based on the actual feature of the Wells turbine in the industry. The rear portion of the design was opened for the drawback movement of air through the rotor. Bearing was attached to the casing for the shaft rotation mechanism. Besides, parts were easy to assemble for the needs of testing. Some mechanical engineering designs were carried out to analyze the conceptual design before the 3D solid modelling design by CATIA. Mechanical engineering design involved the bearing selection, turbine blade and rotor design, and mounting of bearing.

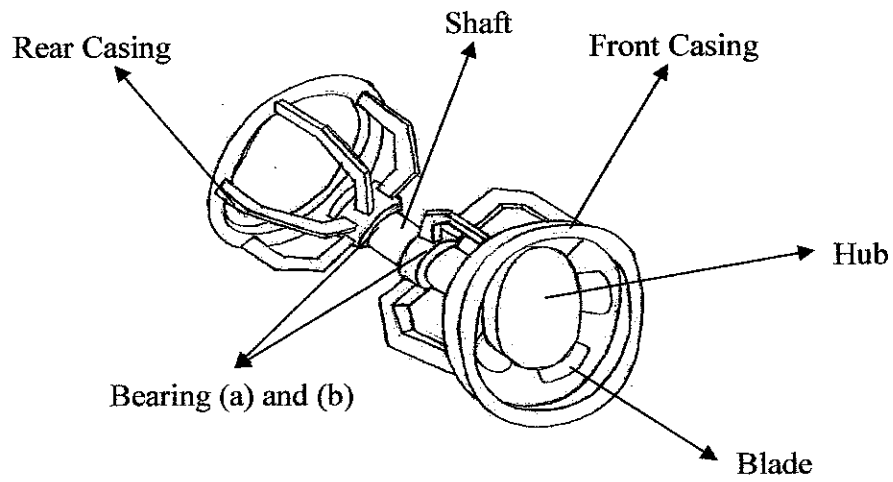


Figure 6: 3D Conceptual design

3.2.2 Conceptual Design Analysis of Wells Turbine Prototype

Figure 7 shows the 2D structure of the prototype. It consists of support and the rotor-shaft parts. Static analysis was carried out to determine the forces acting in the system. In addition, analysis to determine the reaction forces in order to maintain the system in equilibrium. As a result, the analysis data were used as a reference for the 3D solid design in CATIA.

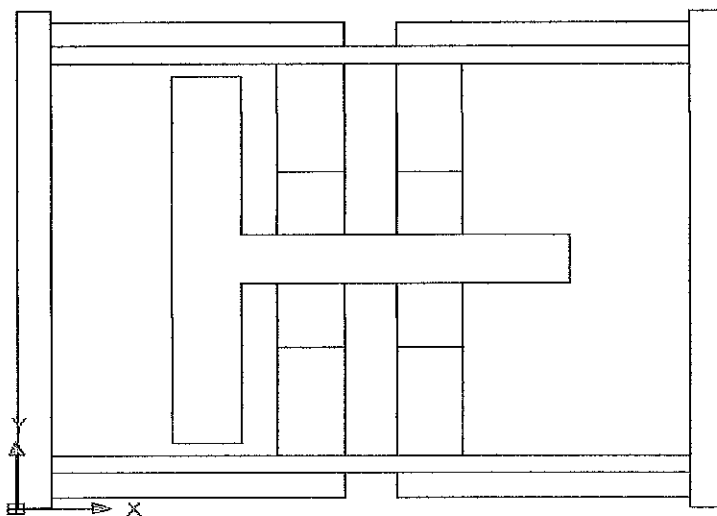


Figure 7: Prototype 2D Structure

Initially, the analysis was focused on the rotor-shaft structure as shown in Figure 8. In the 2D analysis, the centroid was a point defined the geometric centre of an object. This point coincided with the centre of mass or the centre of gravity only if the material composing the body is uniform or homogeneous. The centroid point was the point where the weight of the part acting due to the gravitational attraction forces.

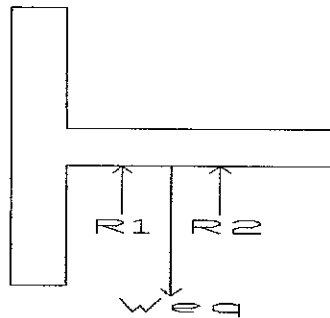


Figure 8: Rotor-shaft 2D Structure

Parts. The part was divided into two segments as shown in the Figure 9. Here the areas were all positives since the 1 and 2 were added together.

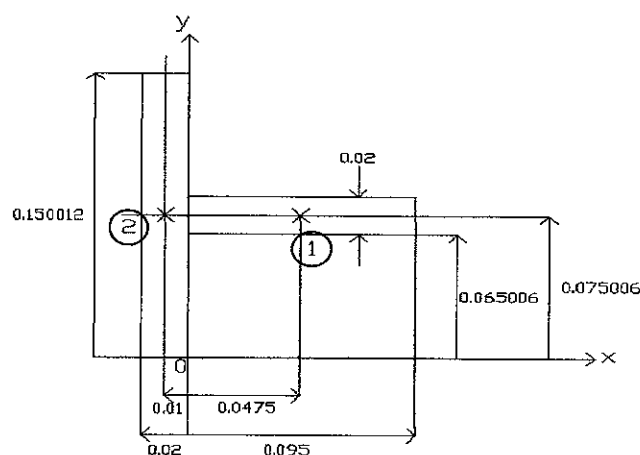


Figure 9: Rotor-shaft Centroid Analysis

Moment Arms. The centroid of each segment was located as indicated in the figure. Note that the \tilde{x} coordinate of 2 was negative.

Summation. Taken the data from the Figure 9, the calculations were tabulated as follows:

Table 1: Centroid calculation of first configuration of rotor-shaft part

| Segment | A (m ²) | \tilde{x} (m) | \tilde{y} (m) | $\tilde{x} A$ (m ³) | $\tilde{y} A$ (m ³) |
|---------|-------------------------------------|-----------------|-----------------|---|--|
| 1 | $0.095 \times 0.02 = 0.0019$ | 0.0475 | 0.075006 | 9.025×10^{-5} | 1.425114×10^{-4} |
| 2 | $0.02 \times 0.150012 = 0.00300024$ | -0.01 | 0.075006 | -3.00024×10^{-5} | 2.25036×10^{-4} |
| | $\sum A = 0.00490024$ | | | $\sum \tilde{x} A = 6.02476 \times 10^{-5}$ | $\sum \tilde{y} A = 3.675474 \times 10^{-4}$ |

$$\bar{x} = \frac{\sum \tilde{x} A}{\sum A} = \frac{6.02476 \times 10^{-5}}{0.00490024} = 0.012295 \text{ m}$$

$$\bar{y} = \frac{\sum \tilde{y} A}{\sum A} = \frac{3.675474 \times 10^{-4}}{0.00490024} = 0.0750056 \text{ m}$$

The centroid of the rotor-shaft system was:

$$\bar{x} = 0.012295 \text{ m} , \bar{y} = 0.0750056 \text{ m}$$

Figure 10 showed the centroid point of the rotor-shaft part. Centroid point was the point where the weight acting.

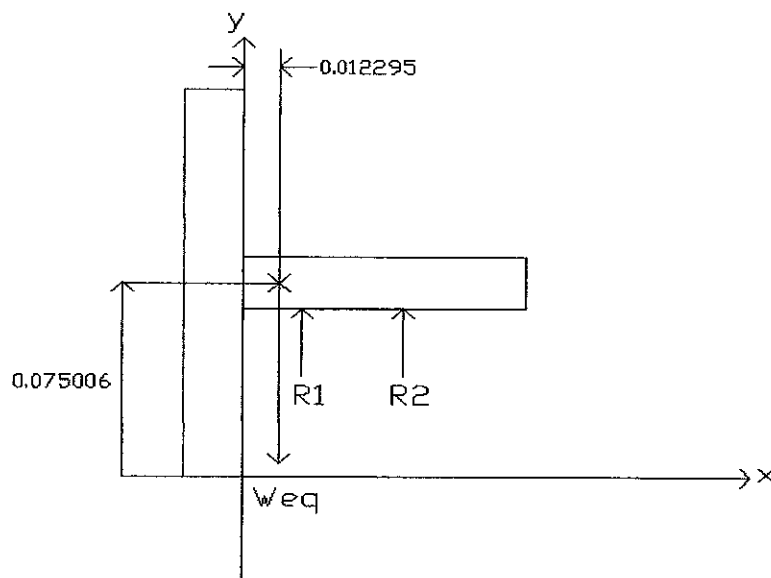


Figure 10: Centroid of rotor-shaft part

Assume Material Used: Polymer-wax

Polymer-wax properties:

Volume = $2.552 \times 10^{-4} \text{ m}^3$

Area = 0.044 m^2

Mass = 0.306 kg

Density = 1200 kgm^{-3}

By referring on Figure 11, R_1 and R_2 were calculated,

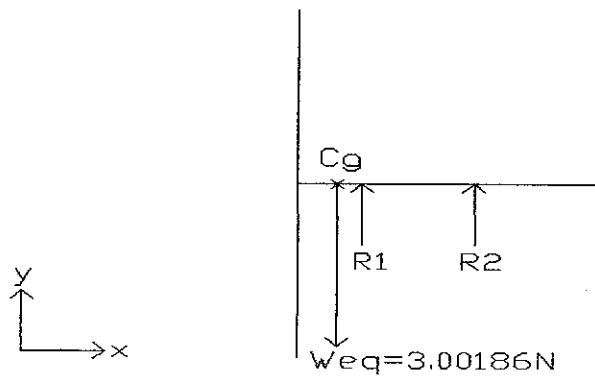


Figure 11: Coplanar Force System of Rotor-shaft Structure

$$\begin{aligned} \uparrow + \sum F_y &= 0, \\ -3.00186 + R_1 + R_2 &= 0 \end{aligned} \quad \text{--(5)}$$

$$\begin{aligned} \text{Counter clockwise} + \sum M_{Cg} &= 0, \\ R_1 (0.027705) + R_2 (0.062705) &= 0 \\ R_2 &= -\frac{R_1 (0.027705)}{0.062705} \\ R_2 &= -0.44183R_1 \end{aligned} \quad \text{--(6)}$$

$$\begin{aligned} \text{Substitute (2) into (1)} \\ -3.00186 + R_1 + R_2 &= 0 \\ -3.00186 + R_1 - 0.44183R_1 &= 0 \\ 0.55817R_1 &= 3.00186 \\ R_1 &= \frac{3.00186}{0.55817} \\ R_1 &= 5.37804 \text{ N} \end{aligned} \quad \text{--(7)}$$

Substitute (7) into (6)

$$\begin{aligned} R_2 &= -0.44183R_1 \\ &= -0.44183 (5.37804) \\ &= -2.37618 \text{ N} \end{aligned}$$

R_2 should be in opposite direction.

Figure 12 showed the exact magnitudes and direction of forces acting on the rotor-shaft structure. Initially, the R_2 was assumed acting in the upward direction. After the force equilibrium analysis of forces in y -direction, it showed that the R_2 acting in the downward direction of y -axis.

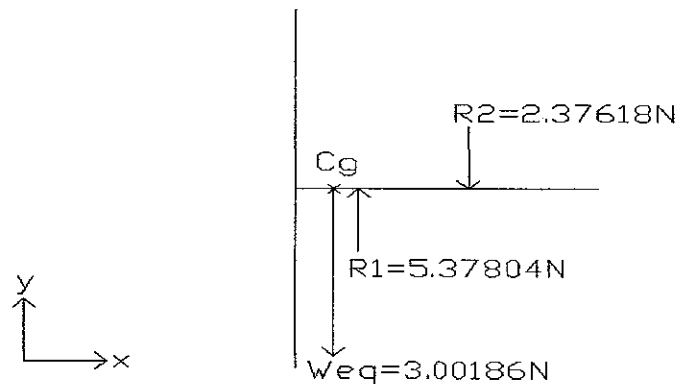


Figure 12: Coplanar Force Magnitude and Direction on Rotor-shaft Structure

3.2.3 Bearing Selection

Figure 13 showed the Deep Groove Ball Bearing. There were parameters involved in the consideration of Deep Groove ball bearing selection process. Ball bearings were selected to accept the thrust. The life goal was 10kh, with reliability to equal 0.99. The application factor was to be 1.2.

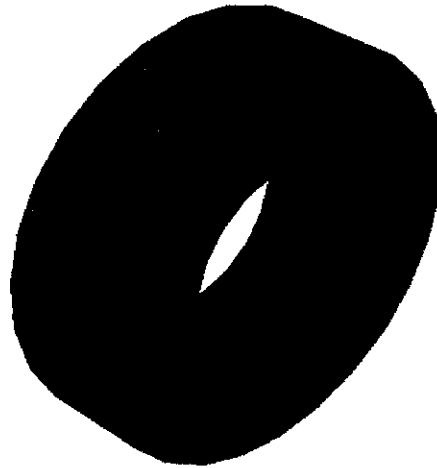


Figure 13: Deep Groove Ball Bearing

Deep Groove Ball Bearing Selection

$$F_r = \sqrt{(364.30^2 + 303.85^2)}$$

$$= 474.37N$$

$$AF = 1.2$$

$$F_a = 351.33N$$

$$R = 0.99$$

$$x_D = \frac{L}{L_{10}} = \frac{60L_D n_D}{60L_R n_R} = \frac{60(10000)656}{10^6} = 393.6 \text{ Multiple of rating life}$$

Table 2 (refer Appendix II) : At first approximation, take the middle entry from table.

$$X_2 = 0.056 \quad , \quad Y_2 = 1.63$$

$$\frac{F_e}{VF_r} = X_2 + Y_2 \frac{F_a}{VF_r}$$

$$\frac{F_e}{VF_r} = 0.56 + 1.63 \frac{351.33}{(1)(474.37)} = 1.77$$

$$F_e = 1.77VF_r = 1.77(1)(474.37) = 0.8396kN$$

$$C_{10} = 1.2(0.8396) \left[\frac{393.6}{0.02 + 4.439(1 - 0.99)^{\frac{1}{1.483}}} \right]^{\frac{1}{3}} = 12.25kN$$

From Table 3 (refer Appendix II), Deep Groove Ball Bearing 02 - 20 mm has $C'_{10} = 12.7kN$, $C_0 = 6.20kN$.

$$\frac{F_a}{C_0} = \frac{351.33 \times 10^{-3}}{6.20} = 0.057$$

which makes e from Table 2 (refer Appendix II) approximately 0.26,

$$\text{Now } \frac{F_a}{VF_r} = \frac{351.33}{(1)(474.337)} = 0.74, \text{ which is greater than } 0.24$$

Find Y_2 by interpolation,

| | | |
|-------------|-------|--|
| F_a / C_0 | Y_2 | |
| 0.056 | 1.71 | $\frac{0.057 - 0.056}{0.070 - 0.056} = \frac{Y_2 - 1.71}{1.63 - 1.71}$ |
| 0.057 | Y_2 | |
| 0.070 | 1.63 | $Y_2 = 1.70$ |

$$\frac{F_e}{VF_r} = 0.56 + 1.70 \frac{351.33}{(1)(474.37)} = 1.819$$

$$F_e = 1.819VF_r = 1.819(1)(474.37) = 0.8629kN$$

The prior calculation for C_{10} changes only in F_e , so

$$C_{10} = \frac{0.8629}{0.8396}(12.25) = 12.60kN$$

From Table 3 (refer Appendix II) a Deep Groove Ball Bearing 02 - 20 mm has $C_{10} = 12.7kN, C_0 = 6.20kN$

From the Table 3 (refer Appendix II) a Deep Groove Ball Bearing 02 - 20 mm was still selected, so the iteration was complete.

Therefore, a Deep Groove ball bearing 02-20 mm was a suitable type of bearing that can withstand the thrust and radial load applied on the system.

3.2.4 Turbine Blade and Rotor Design

Turbine blade was based on lift, the emphasis of blade that was specifically designed to generate lift while keeping the drag at a minimum. For devices that were intended to generate lift such as turbine blade, the contribution of viscous effect to lift was usually negligible since the bodies were streamlined, and wall shear was paralleled to the surfaces of such devices and thus nearly normal to the direction of lift. The formula shown was a NACA 4-Digit generator.

$$y=(t/0.2)*(0.2969*(x)^{(0.5)}-0.126*(x)-0.3516*(x)^{(2)}+0.2843*(x)^{(3)}-0.1015*(x)^{(4)})$$

Table 4, Table 5 and Figure 14 showed the profile of the desired design that was fabricated by using Rapid Prototyping (RP). The turbine rotor adopted in the design was shown in Figure 2. The geometry details of turbine rotor shown in Table 5.

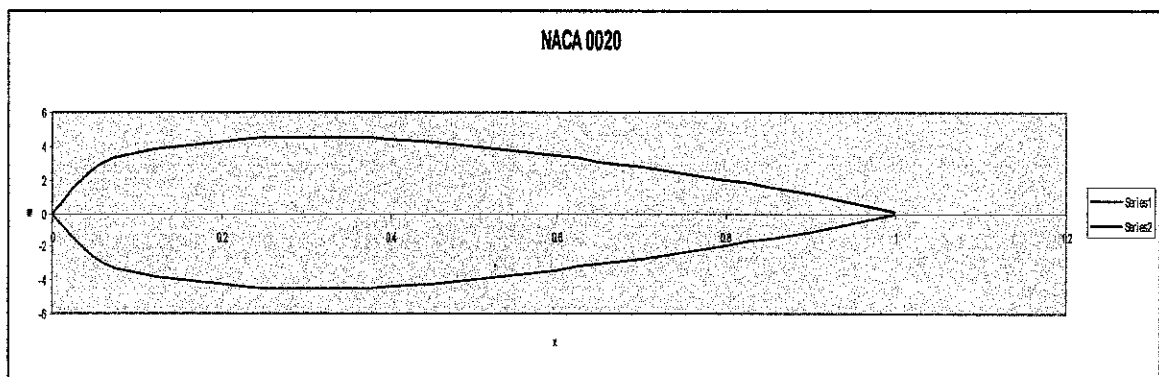


Figure 14: NACA 0020 Profile

Table 4: Profile of the NACA 0020

| x | y(positive) | y(negative) |
|------|-------------|--------------|
| 0 | 0 | 0 |
| 0.05 | 2.666014262 | -2.666014262 |
| 0.1 | 3.512077818 | -3.512077818 |
| 0.15 | 4.008870165 | -4.008870165 |
| 0.2 | 4.303157243 | -4.303157243 |
| 0.25 | 4.455931641 | -4.455931641 |
| 0.3 | 4.50129498 | -4.50129498 |
| 0.35 | 4.46146366 | -4.46146366 |
| 0.4 | 4.352258136 | -4.352258136 |
| 0.45 | 4.185552505 | -4.185552505 |
| 0.5 | 3.9705189 | -3.9705189 |
| 0.55 | 3.714320754 | -3.714320754 |
| 0.6 | 3.422526799 | -3.422526799 |
| 0.65 | 3.099372105 | -3.099372105 |
| 0.7 | 2.747930035 | -2.747930035 |
| 0.75 | 2.370229673 | -2.370229673 |
| 0.8 | 1.967338485 | -1.967338485 |
| 0.85 | 1.539422013 | -1.539422013 |
| 0.9 | 1.085787954 | -1.085787954 |
| 0.95 | 0.60491935 | -0.60491935 |
| 1 | 0.0945 | -0.0945 |

Table 5: Geometric details of rotor

| | |
|------------------------------|-----------------|
| Tip Diameter, D_t | 150 mm |
| Hub Diameter, D_h | 97.5 mm |
| Hub/Tip Ratio | $97.5/150=0.65$ |
| Span, b | 30 mm |
| Chord, c | 37.5 mm |
| Number of Blades | 6 |
| Solidity (chord/blade space) | 0.67 |
| Aspect Ratio, AR (b/c) | 0.7 |
| Mean Radius, r_m | 123.75 mm |

3.2.5 3D Solid Modelling Wells Turbine Prototype

The 3D drawing as shown in Figure 15 was drawn by using CATIA software. The drawing showed the detailed of the components in the prototype. Components involved were the support, rotor-shaft and bearing. The drawing was guidance in the assembly

process. Appendix II showed the detailed Fabrication Drawing of each part. Dimensions and sizes were all detailed specified in the drawing to guide in the machining process further.

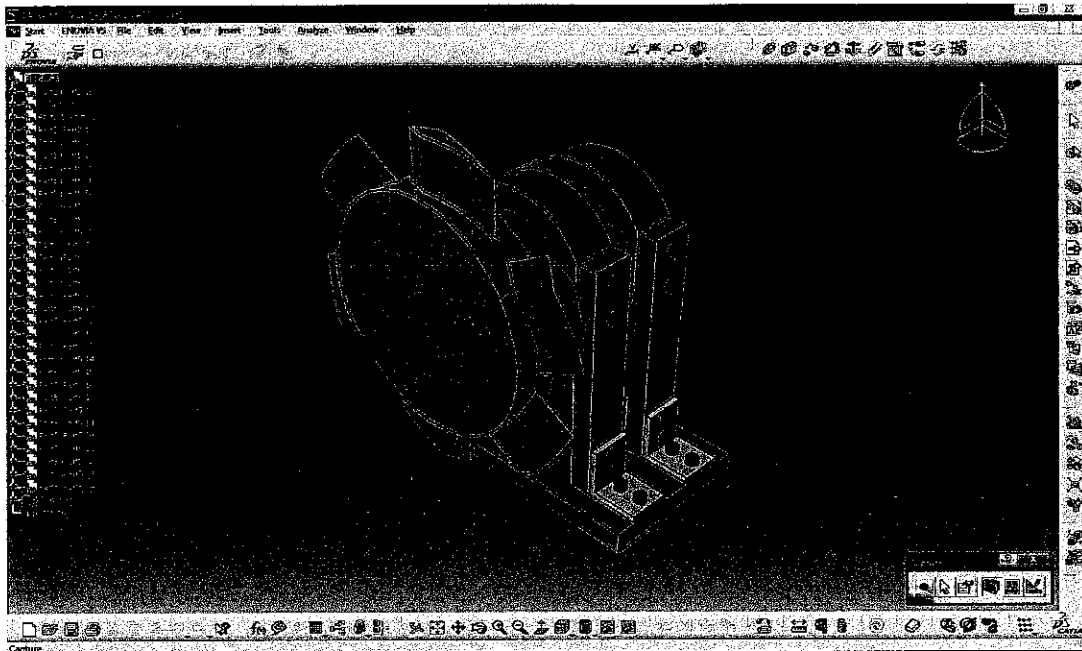


Figure 15: Assembly Drawing of Prototype Parts

3.3 Prototype Wells Turbine Prototyping and Fabrication

3.3.1 Multi Jet Modeling (MJM) Machine Working Principle

Figure 16 showed the Multi Jet Modeling (MJM), also known as Thermojet (TJ). It was a quick rapid prototyping process used for concept modeling. The system generated wax-like plastics models which were less accurate than stereolithography. The machine used a wide area head with multiple spray nozzles. These jetting heads sprayed tiny droplets of melted liquid material which cooled and hardened on impact to form the solid object. The process was commonly used for creating casting patterns for jewelry industry and other precision casting applications. The standard data interfaced between CAD software and the machines was the STL file format. A STL file approximated the

shape of a part or assembly using triangular facets. Smaller facets produced a higher quality surface.



Figure 16: Multi Jet Modelling (MJM)

The basic methodology for all current rapid prototyping techniques can be summarized as follows:

1. A CAD model was constructed, and then converted to STL format. The resolution can be set to minimize stair stepping.
2. The RP machine processed the .STL file by creating sliced layers of the model.
3. The first layer of the physical model was created. The model was then lowered by the thickness of the next layer, and the process was repeated until completion of the model.
4. The model and any supports were removed. The surface of the model was then finished and cleaned.

3.3.2 Material Use in Multi Jet Modeling (MJM)

TJ88 and TJ2000 were TJ materials. TJ88 was harder but more brittle. Both materials come in 3 colors - neutral (cream), grey or black. UTP laboratory used the TJ88 Thermojet material. Known as a wax co-polymer, it was a modified wax with a melting point around 70°C. High cleanliness was required to ensure the fine jets were not blocked. One substantial disadvantage of the Thermojet was the high cost of wax.

3.3.3 Rotor-shaft by Rapid Prototyping (RP) Process

The 3D solid modelling of the rotor-shaft which was in the CATpart format was converted into STL format. This STL format was the format understood by the Thermojet (TJ) machine. Initially, the orientation of 3D solid modelling was set up for the purpose of reducing wasting of the material. The best orientation was selected as shown in the Figure 17 was the hub of the rotor facing the plate. The process was started by developing the support material was at the lower portion attached with the plate and the part. The process took about 12 hours to produce the part. After the fabrication process, the part went into post processing to remove the support material. The post processing methods used were freezing method and spraying method.

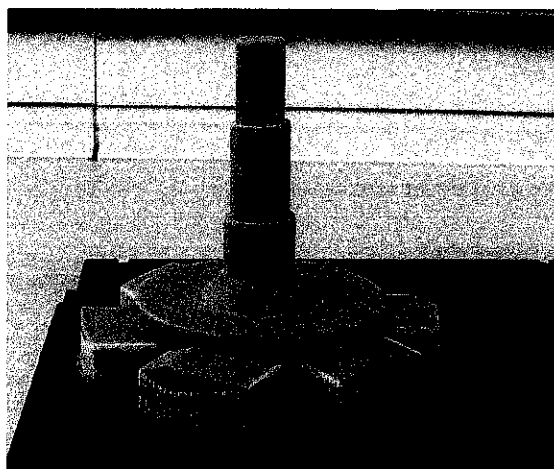


Figure 17: After Rapid Prototyping (RP) Process

3.3.4 Manufacturing Processes of Support Structure

The completed fabrication drawing was used as a reference for manufacturing processes of parts. Initially, this process started with the material preparation by referring on the fabrication drawing. All the required materials were supplied by UTP Manufacturing Laboratory.

In support structure manufacturing process, there were some machining processes involved. There were measuring, cutting, squaring, drilling, boring and milling. Different machining processes involved for each part. Initially, the aluminium plates were measured based on the required dimension as stated in the fabrication drawing. Steel rule and marker were used to measured and marked the dimension and length needed. Figure 18 showed the material preparation.

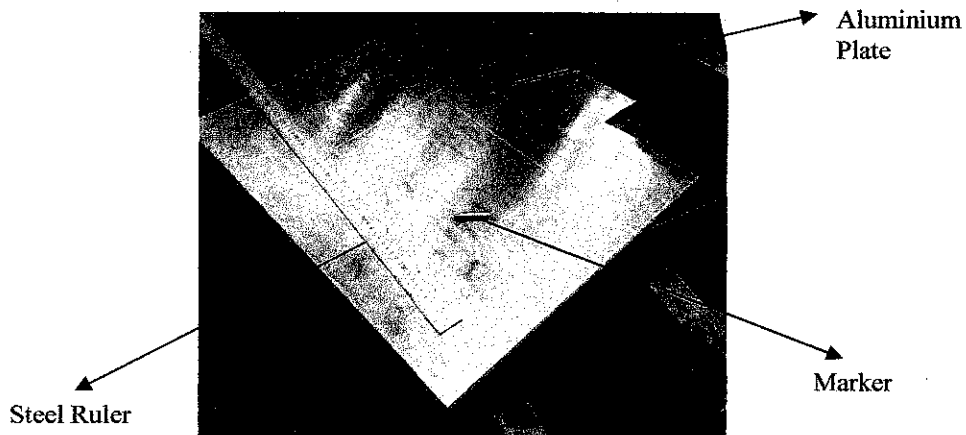


Figure 18: Material preparation

After completed measuring process, the material was cut into small pieces by using particular cutting machine. Figure 19 showed the Linear Hack Saw Machine that was used in material cutting process.

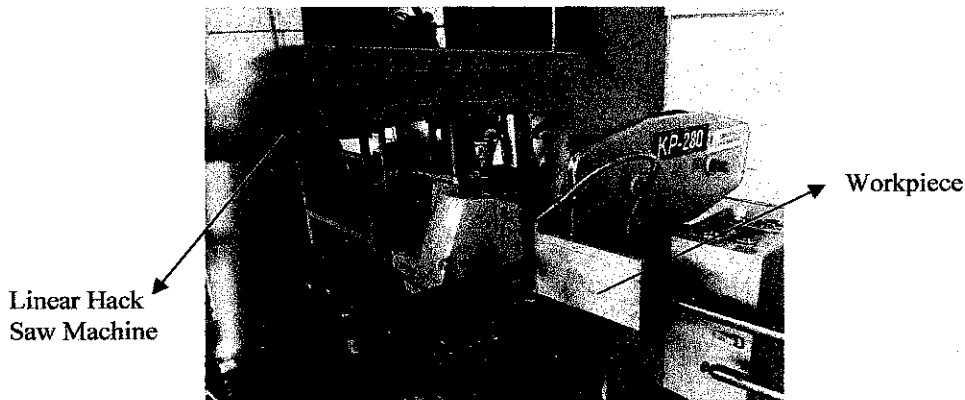


Figure 19: Linear Hack Saw Machine

Standard Operation Procedure of Linear Hack Saw Machine.

Before operation:

1. Make sure the machine is in good condition.
2. Ensure safety and wear appropriated PPE prior to operate the machine.

How to operate:

1. Turn ON main power supply.
2. Turn ON machine power at control panel. Adjust the blade release timer according to workpiece length.
3. Press stop button to lift the hack saw blade at the highest peak. Place the workpiece inside the rise and clamp the workpiece firmly and adjust the length of the workpiece to the desired length.
4. Open coolant valve and press start button to start the cutting process.
5. Machine will automatically stop after cutting blade reaches the lower limit.
6. Press down stop button to lift up back the cutting blade. Unclamp the rise to remove the workpiece.

After operation:

1. Switch off machine by turn off the stop button at control panel and main power supply located beside the machine.

2. Housekeeping

In addition, squaring process was needed to square the material plate. The purposed was to remove the burr at the material edge, to reduce the surface roughness and to get the desired dimension of the plate. The reference surface of the dimension was given one diamond symbol; meaning the accuracy was required. The referenced surface was used for hole drill, boring and cutting process. The Conventional Milling Machine used in squaring process was face milling.

Figure 20 showed the cutter was mounted on a spindle having an axis of rotation perpendicular to the workpiece surface and removed material. The cutter rotated at a rotational speed N , and the workpiece moved along a straight path at a linear speed v . When the cutter rotated, the operation was climb milling; when it was in the opposite direction, the operation was conventional milling. The cutting teeth, such as carbide inserts, were mounted on the cutter body.

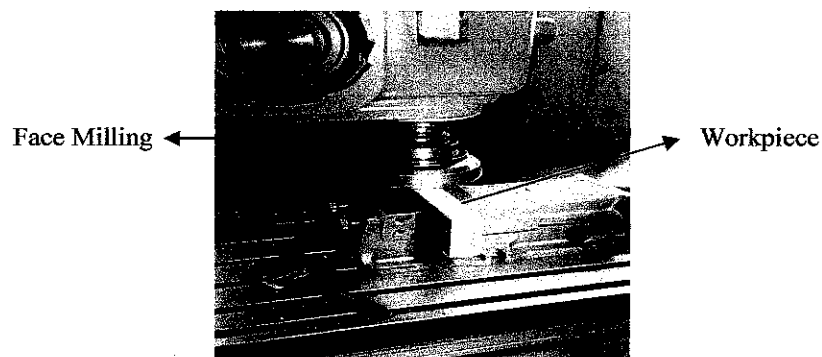


Figure 20: Squaring process using Conventional Milling Machine

CNC Milling machine tools were versatile and capable of milling, drilling, boring, and tapping with repetitive accuracy. Also available were profile milling machines, which have five axes of movement; note the three linear and two angular movements of the machine components.

Figure 21 showed that the CNC Milling was used for boring the bearing mounting's part. Programming language of G-code and M-code were required to command the machine to produce the desired product. In addition, this machine can read the 3D solid modelling that has been drawn. Therefore, from the 3D solid modelling displayed in the computer, the computer numerical automatically generate the codes. Hence, the machine started the machining process.

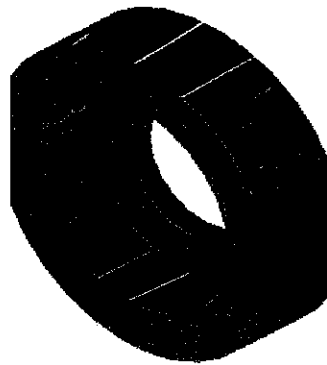


Figure 21: Boring of Bearing Mounting by CNC Milling

3.3.5 Parts Assembly Process

Assembly process was one process ahead after the manufacturing and fabrication processes. This process was merging and combining each single part to become a completed product that can be used for other applications afterwards. Assembly process also one biggest process that required machine or special tools as well as specialist to assemble the parts involved.

In this project, Wells turbine prototype parts were assembled to become a complete build unit of the prototype. The prototype was used for testing of the Rapid Prototyping (RP) rotor-shaft in the wind tunnel.

In the assembly process, Figure 22 below was a very important guide. The drawing would be the reference to ensure that each part was assembled accordingly based on the sequence without interfering to each other. In addition, the drawing was also used to check the accuracy of the part met the design requirement. All the problems occurred were highlighted and was corrected in order to maintain the accuracy of the Wells turbine prototype. Figure 23 showed the completed build unit of the Wells turbine prototype.

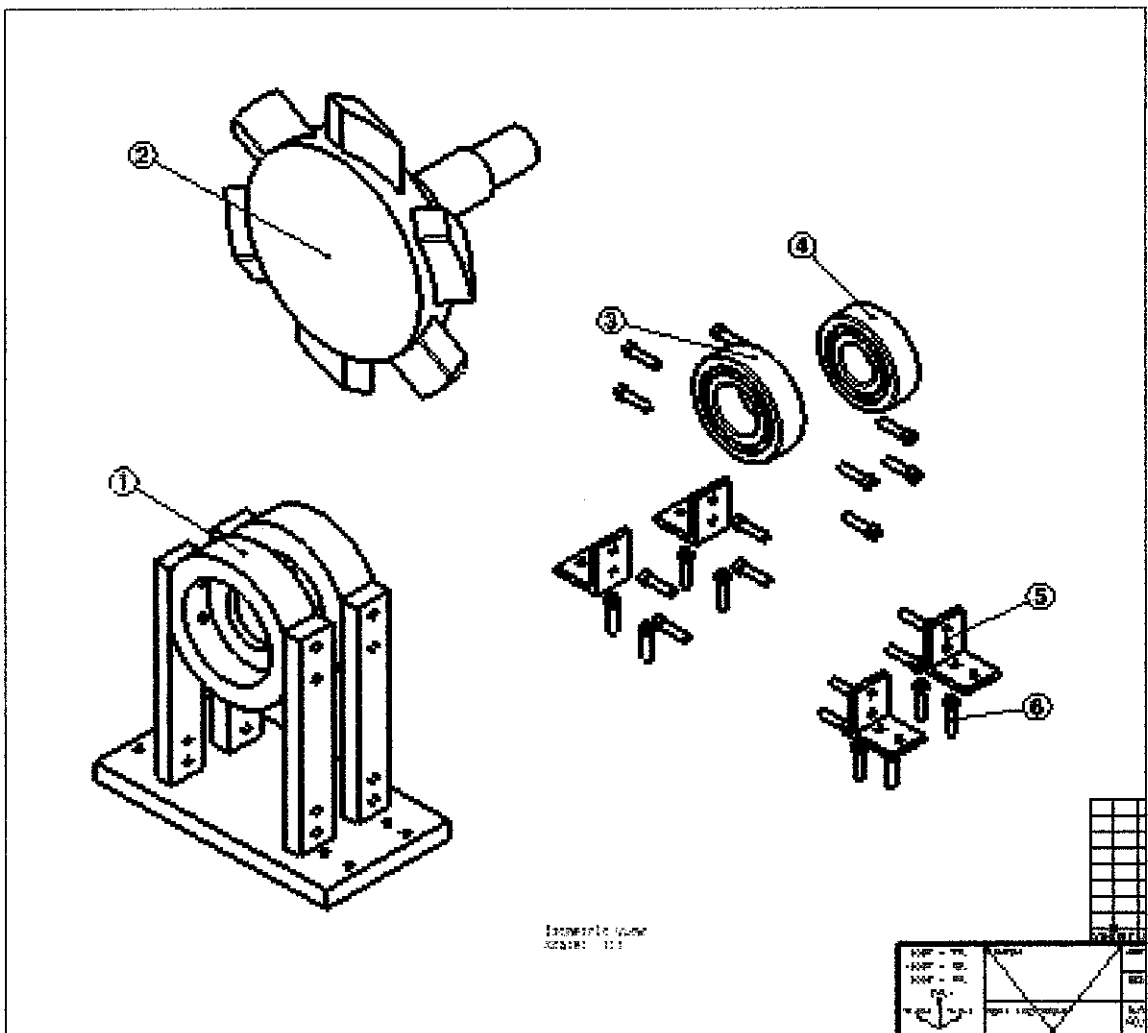


Figure 22: 2-Dimensional Assembly Drawing

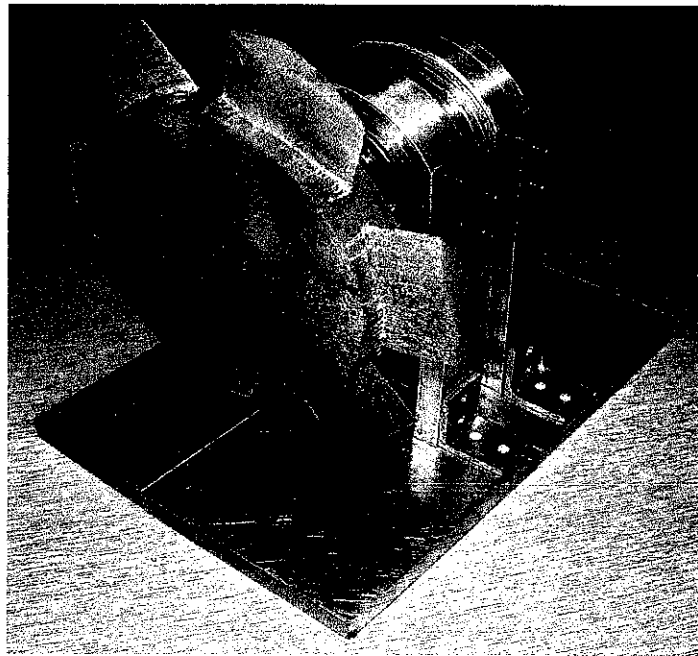


Figure 23: Wells Turbine Prototype

Procedure of the part assembly process:

1. Assembled the bearing mounting houses with the stands by using the M6 bolt.
2. Placed the bearings inside the bearing mounting houses.
3. Assembled the stands with the base by using L-bracket and M6 bolt.
4. Placed the rotor-shaft inside the bearing inner diameter.

3.4 Prototype Wells Turbine Testing

Wind tunnel was used to test the prototype. Wind tunnel testing parameters were manipulated in order to achieve the objectives of the project.

In the testing process, the prototype was tested in the wind tunnel. The testing was to test the Rapid Prototyping (RP) part which was the rotor-shaft. Two (2) configurations were tested. The varied wind tunnel parameter was the air velocity. Therefore, it was used to identify initial wind velocity required to make the rotor rotate. The air velocity kept increasing until the rotor reached the steady state where the increasing of air velocity did

not affect the revolution per minute (rpm) of the rotor. It means that, the rotor had reached the maximum rpm of the rotation.

3.5 Analysis on the Results and Findings

This was to analyze the result obtained from the testing. Base on the results, therefore, discussion, recommendation and conclusion were made.

CHAPTER 4

RESULTS AND DISCUSSION

4.1 Testing Failure for First Configuration

During the testing in the wind tunnel, the first configuration failed and the rotor did not rotate. This problem might be due to either design or fabrication error. Based on the study, the rotor which was produced by the RP process did not rotate due to the blade design problem. It was observed that the blade was not following the NACA 0020 airfoil design specification. Therefore, corrective was done to solve the problem. Figure 24 below showed the blade design problem.

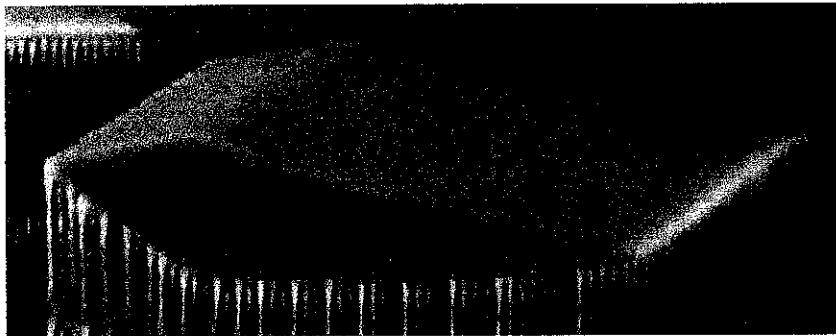


Figure 24: Blade of first configuration

Design change and modification were carried out to produce new rotor-shaft configuration which follows the NACA 0020 airfoil design specification. The new rotor-shaft configuration was produced and follows procedures from the conceptual design until the fabrication process.

4.2 Design of Second Configuration

The study was focused on the new rotor-shaft part as shown in Figure 25. In the 2D analysis, the centroid was a point which defines the geometric midpoint of an entity. This point coincides with the centre of mass or the centre of gravity only if the material composing the body is uniform or homogeneous. The centroid point was the point where the weight of the part acting due to the gravitational attraction forces.

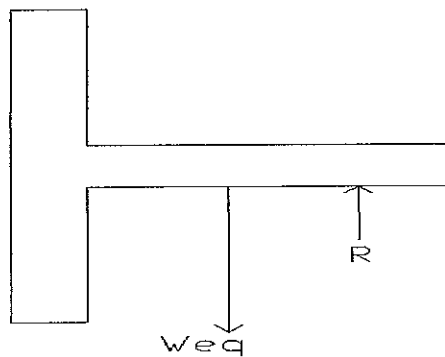


Figure 25: Rotor-shaft 2D part

Parts. The part was divided into two segments as shown in the Figure 26. Here the areas were all positives since the 1 and 2 were added together.

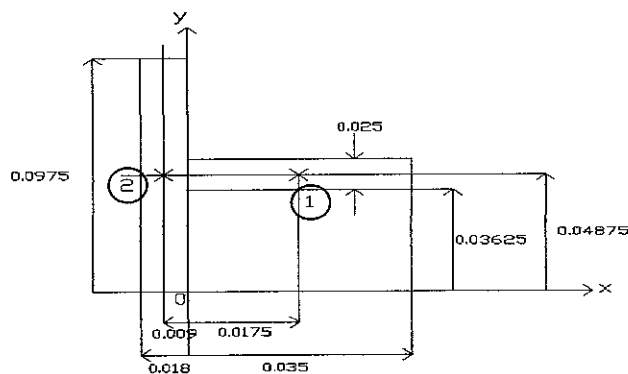


Figure 26: Rotor-shaft Centroid Analysis

Moment Arms. The centroid of each segment was located as indicated in the figure. Note that the \tilde{x} coordinate of 2 was negative.

Summation. Taken the data from the Figure 26, the calculations were tabulated as follows:

Table 6: Centroid calculation of new rotor-shaft part

| Segment | A (m ²) | \tilde{x} (m) | \tilde{y} (m) | $\tilde{x} A$ (m ³) | $\tilde{y} A$ (m ³) |
|---------|---------------------------|-----------------|-----------------|--|--|
| 1 | 0.035 x 0.025 = 0.000875 | 0.0175 | 0.04875 | 1.53125 x 10 ⁻⁵ | 4.265625 x 10 ⁻⁵ |
| 2 | 0.018 x 0.0975 = 0.001755 | -0.009 | 0.04875 | -1.5795 x 10 ⁻⁵ | 8.555625 x 10 ⁻⁵ |
| | $\sum A = 0.00263$ | | | $\sum \tilde{x}A =$ -4.825 x 10 ⁻⁷ | $\sum \tilde{y}A =$ 1.282125 x 10 ⁻⁴ |

$$\bar{x} = \frac{\sum \tilde{x}A}{\sum A} = \frac{-4.825 \times 10^{-7}}{0.00263} = -0.00018346 \text{ m}$$

$$\bar{y} = \frac{\sum \tilde{y}A}{\sum A} = \frac{1.282125 \times 10^{-4}}{0.00263} = 0.04875 \text{ m}$$

The centroid of the rotor-shaft system was:

$$\bar{x} = -0.00018346 \text{ m} , \bar{y} = 0.04875 \text{ m}$$

Figure 27 showed the centroid point of the rotor-shaft part. Centroid point was the point where the weight acting.

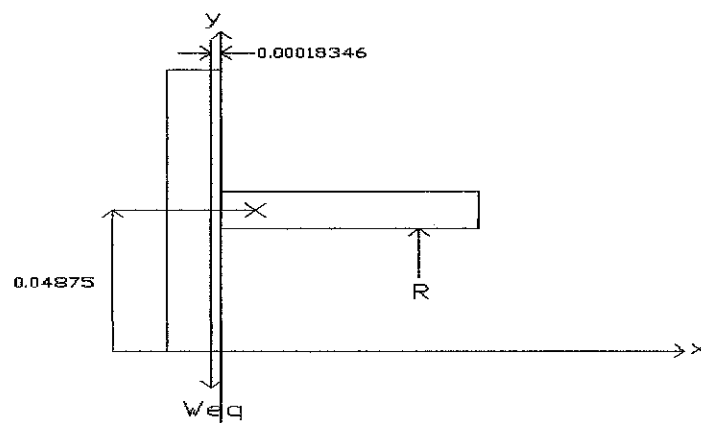


Figure 27: Centroid of Rotor-shaft Part

Assume Material Used: Polymer-wax

Polymer-wax properties:

Volume = $1.636 \times 10^{-4} \text{ m}^3$

Area = 0.041 m^2

Mass = 0.13906 kg

Density = 850 kgm^{-3}

By referring Figure 28, R was calculated,

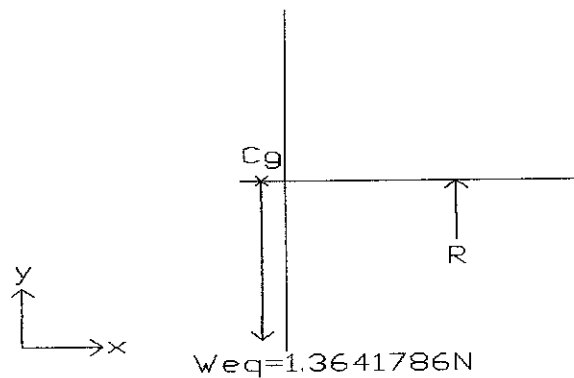


Figure 28: Coplanar Force System of Rotor-shaft Part

$$\begin{aligned} \uparrow + \sum F_y &= 0, \\ -0.13906(9.81) + R &= 0 \\ R &= 1.3641786 \text{ N} \end{aligned}$$

Figure 29 showed the exact magnitudes and direction of forces acting on the rotor-shaft part. After the force equilibrium study of forces in y-direction, it showed that the R acting in the upward direction of y-axis.

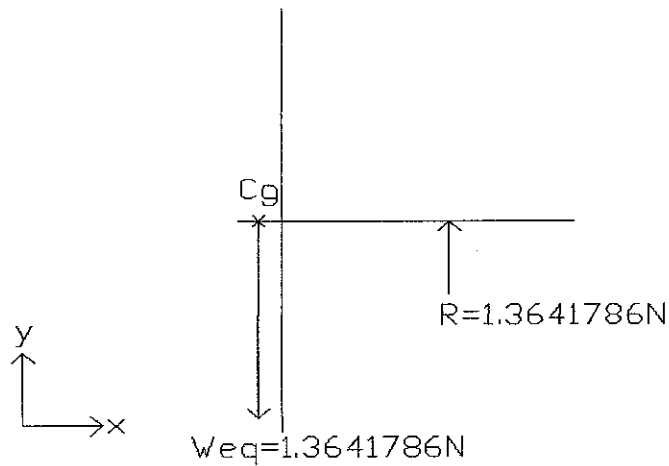


Figure 29: Coplanar Force Magnitude and Direction on Rotor-shaft Part

4.3 3D Solid Modelling Design by CATIA

Figure 30 below showed the new configuration of the prototype where the design was simplified. The drawing showed the completed of the components in the prototype. Components involved were the rotor-shaft, bearing and rod. The drawing was used as guided in the assembly process. Appendix II showed the detailed Fabrication Drawing of each part. Dimensions and sizes were all completely specified in the drawing to help in the machining process.

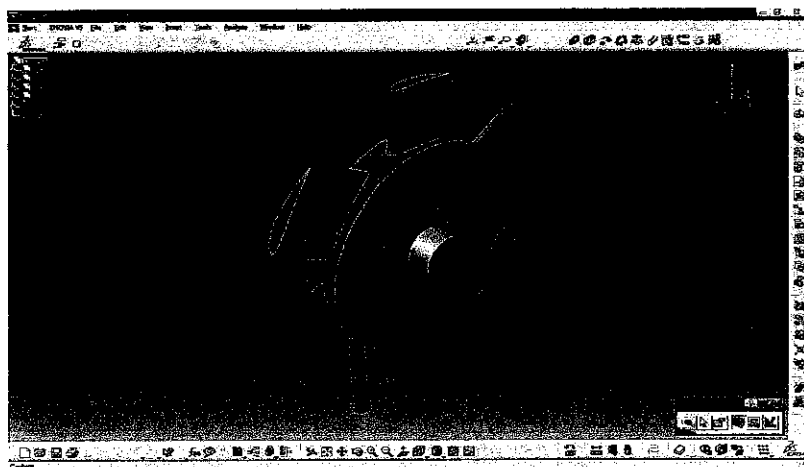


Figure 30: Assembly Drawing of Prototype Parts

4.4 Blade Design Modification

Figure 31 showed the new blade design which follows the NACA 0020 specification. Table 7 stated the coordinate of the new blade design.

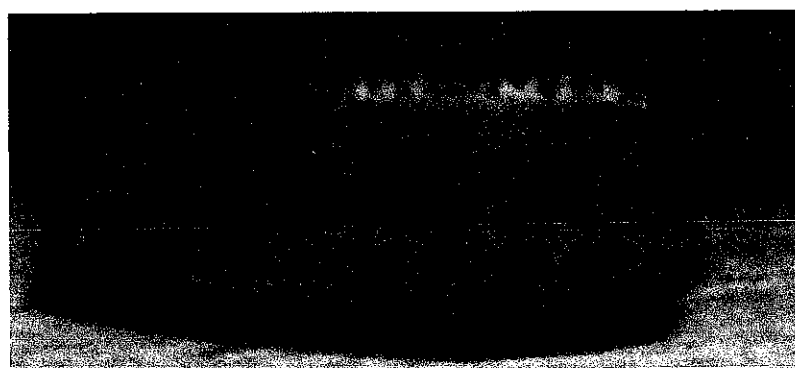


Figure 31: Blade of new configuration

Table 7: Profile of the NACA 0020 for new configuration

| x | +y | -y |
|--------|--------|---------|
| 0.000 | 0 | 0 |
| 1.875 | 2.3230 | -2.3230 |
| 3.750 | 2.9809 | -2.9809 |
| 5.625 | 3.3672 | -3.3672 |
| 7.500 | 3.5960 | -3.5960 |
| 9.375 | 3.7147 | -3.7147 |
| 11.250 | 3.75 | -3.75 |
| 13.125 | 3.7191 | -3.7191 |
| 15.000 | 3.6342 | -3.6342 |
| 16.875 | 3.5045 | -3.5045 |
| 18.750 | 3.3373 | -3.3373 |
| 20.625 | 3.1381 | -3.1381 |
| 22.500 | 2.9112 | -2.9112 |
| 24.375 | 2.6600 | -2.6600 |
| 26.250 | 2.3867 | -2.3867 |
| 28.125 | 2.0930 | -2.0930 |
| 30.000 | 1.7797 | -1.7797 |
| 31.875 | 1.4470 | -1.4470 |
| 33.750 | 1.0943 | -1.0943 |
| 35.625 | 0.7204 | -0.7204 |
| 37.500 | 0.3235 | -0.3235 |

4.5 Result Analysis

Commercial software, FLUENT 6, was used for the numerical analysis. The steady state, three-dimensional Reynolds-averaged Navier Stokes equations were discretized by the finite volume method. The rotating frame of references fixed to turbine rotor was adopted.

The structured, hexahedral grid was used and the total number of grids was approximately 250,000. Nonslip boundary conditions were used for the hub surface, the pressure and suction side of rotor surfaces. Periodic boundary conditions were used for the surface of circumferential sides. Inlet velocities were given on the upstream boundary, while the static pressures were given on the downstream boundary.

Figure 32 showed that the relationship between the lift and drag coefficient of NACA 0020 with the angle of attack, α at Reynold number of 10^5 . Based on the Wells turbine principle, the blade has been originally set up normal to the direction of the air flow which was at 90° angle of attack. Refer to the graph above, at 90° angle of attack, the C_L was 0.06 and the C_D was 1.42. It means that the blade had no twist therefore the flow-angle of the air was equal to the angle of attack, α . It was observed that the turbine has too large angles meaning that the blade was operating mostly in the stalled region.

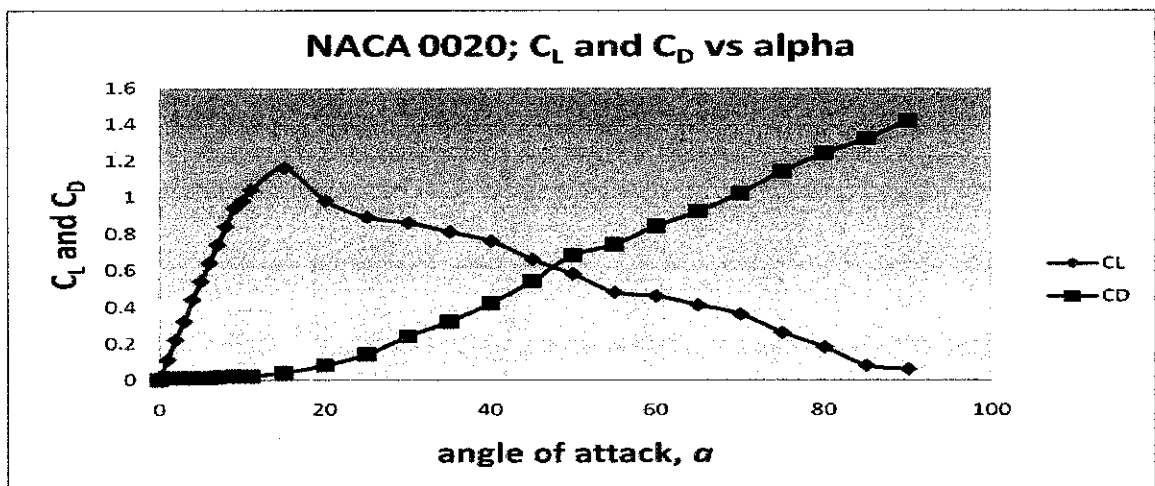


Figure 32: NACA 0020, Lift Coefficient, C_L and Drag Coefficient, C_D vs alpha

As the angle of attack, α increased, lift increased until stall (a situation during which an angle of attack becomes so large that the air flow no can longer flow smoothly, or laminar, across the profile) of NACA 0020 occurred at angle of attack 15° . It showed that after this angle, the C_L started decreased while C_D increased. Therefore, drag coefficient was greater than the lift coefficient during the operation of the Wells turbine. It proved that, the turbine required some initial force to start the rotation of the rotor. The Wells turbine consumed some amount of energy before it started to generate useful energy.

Figure 33 showed the relationship between the lift and drag force of the NACA 0020 at 90° angle of attack by varying the air velocity in the wind tunnel. It showed that, at the beginning of the operation, both forces were zero since there was zero velocity of the air. The air velocity was increased with 5 m/s increment. Curves showed that the slope of the drag force was greater that the slope of the lift force. It means that the drag force was a dominant force acting on the turbine during the operation. The turbine operated in a condition of high drag force which made the turbine less efficient to extract the kinetic energy of the air into mechanical energy of the rotation of the rotor.

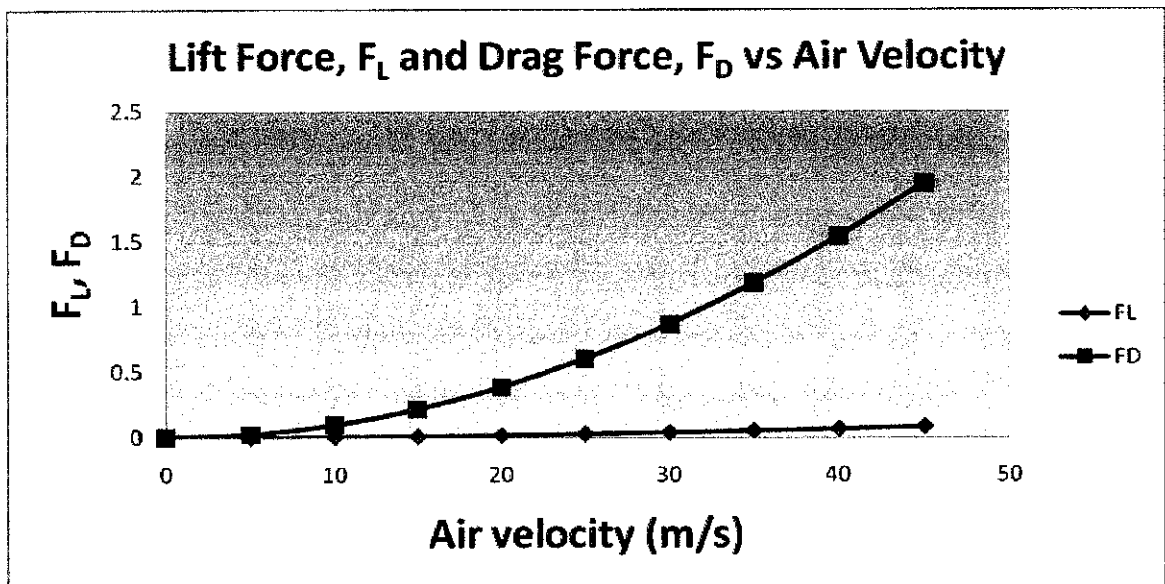


Figure 33: NACA 0020, Lift Force, F_L and Drag Force, F_D vs Air Velocity

Based on the wind tunnel air velocity parameter setting, the allowable maximum air velocity was 60 m/s. It showed that at 40 m/s, the drag force reached at 1.94 N and the lift force was 0.082 N. The lifting was much less than the drag forces. Therefore, it was difficult for lift force to lift the rotor and produce a rotation.

Figure 34 showed that the relationship of the revolution per minute (rpm) of rotor with the varying of the air velocity in the wind tunnel. It showed that, at zero air velocity, the rotor did not rotate since the forces acting on the rotor was zero. This was because the air velocity was the main component that affects the forces based on the equation below.

$$F_L = C_L \frac{1}{2} \rho V^2 A$$

$$F_D = C_D \frac{1}{2} \rho V^2 A$$

F_D = Drag force, N

F_L = Lift force, N

C_L = Lift Coefficient

C_D = Drag coefficient

ρ = Air density= 1.2 kg/m³

V = Air Velocity, m/s

A = Planform area, m²

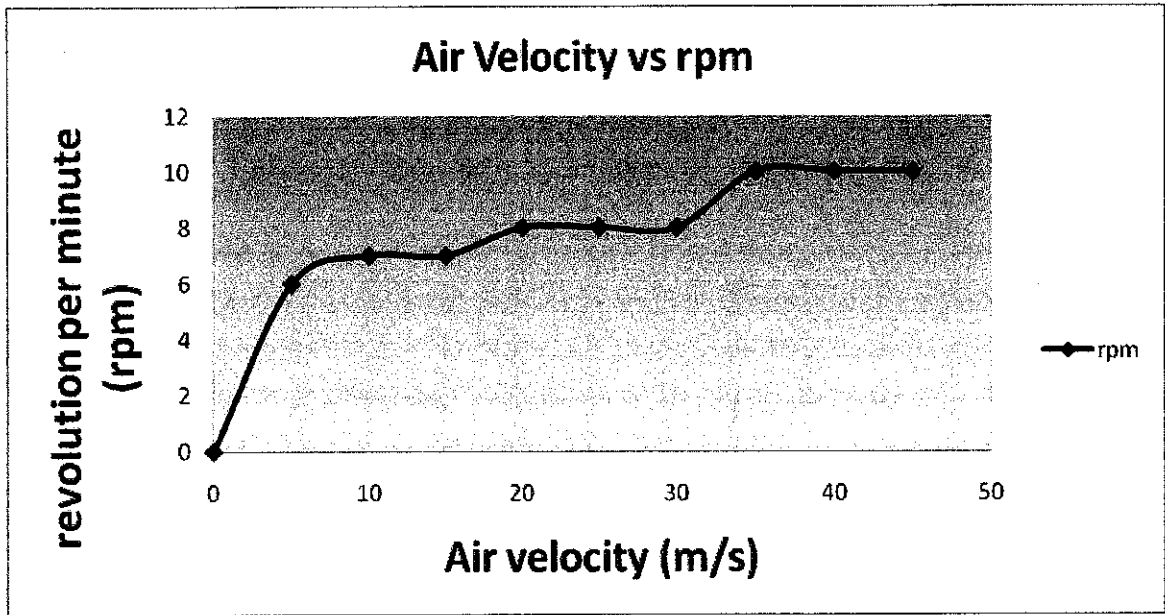


Figure 34: Revolution per minute (rpm) vs Air Velocity

It was observed that, the rotor started to rotate at 6 rpm when the air velocity is equal to 5 m/s. Therefore, based on the objective of the study, the start up air velocity is 5 m/s. As the air velocity was kept increasing with the increment of 5 m/s, the rpm also increased. Besides that, the rotational speed at air velocity of 10 until 15 m/s was 7 rpm. It means that, the rpm was constant while the speed of the air increased from 10 to 15 m/s. The rotational speed of the turbine also exhibited discrete increments when air velocity was increased. For instance at a wind speed between 10 to 15 m/s, the rotor speed is 7 rpm. At an air speed of 20 to 30 m/s, the rotor rotated at 8 rpm while at a wind speed between 35 to 45 m/s, the rotor speed reaches a maximum of 10 rpm.

CHAPTER 5

CONCLUSION AND RECOMMENDATION

Conceptual design of the Wells turbine prototype, static analysis of the support structure and mechanical components designs were carried out. These data were used in the CATIA 3D solid models. Two different rotor configurations were designed and fabricated by using Rapid Prototyping (RP). Each rotor took about 12 hours to be fabricated and the material used was polymer-wax. These two rotors were tested in the wind tunnel. Air velocity was the main variable parameter to analyze the rotor performance. The first rotor configuration failed due to blade design error while the second rotor succeeded and provided significant data. The data were interpreted in a plot of rotational speed (rpm) vs air velocity.

Based on the completed project, there are some improvements that can be applied for future study. In the design stage, further analysis can be carried out such as stress analysis on the critical components such as the rotor which is subjected to cyclic loading and vibration. The simulation tools or software can be used to analyze the condition of the rotor before the actual testing in the wind tunnel. In the failure of first rotor configuration, there were factors that also contributed to the failure such as the usage of polymer-wax. Polymer-wax is heavy, poor surface finish and brittle. Instead of using wind tunnel as a source of the moving air, the enclosed chamber with filled with water can be used to produce the oscillating water column (OWC). The OWC is the main source of moving air which is drives the rotor of the Wells turbine.

In order to improve the smoothness of the project development, Universiti Teknologi PETRONAS (UTP) should provide another RP machine and wind tunnel. This is due to high utilization of these equipments by the students. Therefore, this can help students to complete their work at the specified time.

Recommendations for future work are as follows:

- Compare different RP rotor configurations with varying the number of blades, NACA series, hub-to-tip ratio, chord and span.
- Reduce the weight of RP rotor and install the nose at the hub in order to improve the aerodynamic features and air flow through the turbine.
- Setup oscillating water column (OWC) device, which consists of enclosed chamber and container filled with water. OWC will produce the moving air and drive the rotor. An alternative way in avoiding the difficulty if use the wind tunnel.

REFERENCES

Takao, M, Setoguchi, T, Kinoue, Y and Kaneko, K. 2006, "*Wells turbine with end plate for wave energy conservation*" <<http://www.elsevier.com/locate/oceaneng>>

Cunningham, L., *The Lost Byte Method of Making Wing Rib Templates*, NACA 4-Digit Airfoils for Stunters, Part I

Govardhan, M. and Chauhan, V.S. 2007, *Numerical Studies on Performance Improvement of Self-Rectifying Air Turbine for Wave Energy Conversion*, Department of Mechanical Engineering, India Institute of Technology Madras, India

Tindall, C.E. and Xu, M. 1996, *Optimising a Wells-Turbine-Type Energy System*. IEEE Transaction on Energy Conversion, Vol. 11, No. 3, Dept. of Electrical Engineering, Queen's University of Belfast, UK

Cengel, Y.A. and Cimbala, J.M., 2006, *Fluid Mechanics: Fundamentals and Applications*, Mc Graw Hill International Edition

Grenda, E., 2006, *The Most Important Commercial Rapid Prototyping Technologies at a Glance*

Wright, Paul K., 2001, *21st Century Manufacturing*. New Jersey: Prentice Hall Inc.

Wohlers, T., 2007, *Rapid Prototyping Terms and Description*

http://www.efunda.com/processes/rapid_prototyping/intro.cfm

http://home.att.net/~castleisland/ind_11.htm

APPENDIX I

Gantt chart

Table 2: Equivalent Radial Load Factors for Ball Bearings

Table 3: Dimensions and Load Ratings for Single-Row 02 Series Deep-Groove

| No. | Detail/ Week | 1 | 2 | 3 | 4 | 5 | 6 | 7 | Mid-semester break | | | | | 8 | 9 | 10 | 11 | 12 | 13 | 14 |
|-----|--|---|---|---|---|---|---|---|--------------------|--|--|--|--|---|---|----|----|----|----|----|
| 1 | Selection of Project Topic | | | | | | | | | | | | | | | | | | | |
| 2 | Preliminary Research Work Research base on: • Related books • Information from internet • Related technical reports • Study the working principle of Wells turbine | | | | | | | | | | | | | | | | | | | |
| 3 | Submission of Preliminary Report | | | | ● | | | | | | | | | | | | | | | |
| 4 | Project Work Design of various configurations (CATIA): • Turbine blade • Number of blades | | | | | | | | | | | | | | | | | | | |
| 5 | Submission of Progress Report | | | | | | | | | | | | | | | | | | | |
| 6 | Seminar (compulsory) | | | | | | | | | | | | | | | | | | | |
| 7 | Project work continues Design of various configurations (CATIA): • Turbine blade • Number of blades Rapid Prototyping (Thermojet) Fabrication of: • Turbine components • Various configurations of turbine | | | | | | | | | | | | | | | | | | | |
| 8 | Submission of Interim Report Final Draft | | | | | | | | | | | | | | | | | | | |
| 9 | Oral Presentation | | | | | | | | | | | | | | | | | | | |

● Suggested milestone
■ Process

Suggested Milestone for the First Semester of Final Year Project I

| No. | Detail/ Week | 1 | 2 | 3 | 4 | 5 | 6 | 7 | 8 | 9 | 10 | 11 | 12 | 13 | 14 |
|-----|---|---|---|---|---|---|---|---|---|---|----|----|----|----|----|
| 1 | Project Work Machining Processes: • Measuring • Cutting • Milling • Boring | | | | | | | | | | | | | | |
| 2 | Submission of Progress Report 1 | | ● | | | | | | | | | | | | |
| 3 | Project Work Continue • Assembly process • Functional Testing Parameter • Wind Tunnel Testing • Gather Data | | | | | | | | | | | | | | |
| 4 | Submission of Progress Report 2 | | | | | | | | ● | | | | | | |
| 5 | Seminar (compulsory) | | | | | | | | ● | | | | | | |
| 6 | Project Work Continue • Wind Tunnel Testing • Gather Data | | | | | | | | | | | | | | |
| 7 | Poster Exhibition | | | | | | | | | | ● | | | | |
| 8 | Submission of Dissertation | | | | | | | | | | | | ● | | |
| 9 | Oral Presentation | | | | | | | | | | | | | ● | |
| 10 | Submission of Project Dissertation (Hard Bound) | | | | | | | | | | | | | | ● |

Mid-semester break

● Suggested milestone
■ Process

Suggested Milestone for the First Semester of Final Year Project II

| | | $F_a/VF_r < e$ | | $F_a/VF_r > e$ | |
|-----------|------|----------------|-------|----------------|-------|
| F_a/C_0 | e | X_1 | Y_1 | X_2 | Y_2 |
| 0.014 | 0.19 | 1.00 | 0 | 0.56 | 2.30 |
| 0.021 | 0.21 | 1.00 | 0 | 0.56 | 2.15 |
| 0.028 | 0.22 | 1.00 | 0 | 0.56 | 1.99 |
| 0.042 | 0.24 | 1.00 | 0 | 0.56 | 1.85 |
| 0.056 | 0.26 | 1.00 | 0 | 0.56 | 1.71 |
| 0.070 | 0.27 | 1.00 | 0 | 0.56 | 1.63 |
| 0.084 | 0.28 | 1.00 | 0 | 0.56 | 1.55 |
| 0.110 | 0.30 | 1.00 | 0 | 0.56 | 1.45 |
| 0.170 | 0.34 | 1.00 | 0 | 0.56 | 1.31 |
| 0.280 | 0.38 | 1.00 | 0 | 0.56 | 1.15 |
| 0.420 | 0.42 | 1.00 | 0 | 0.56 | 1.04 |
| 0.560 | 0.44 | 1.00 | 0 | 0.56 | 1.00 |

Table 2: Equivalent Radial Load Factors for Ball Bearings

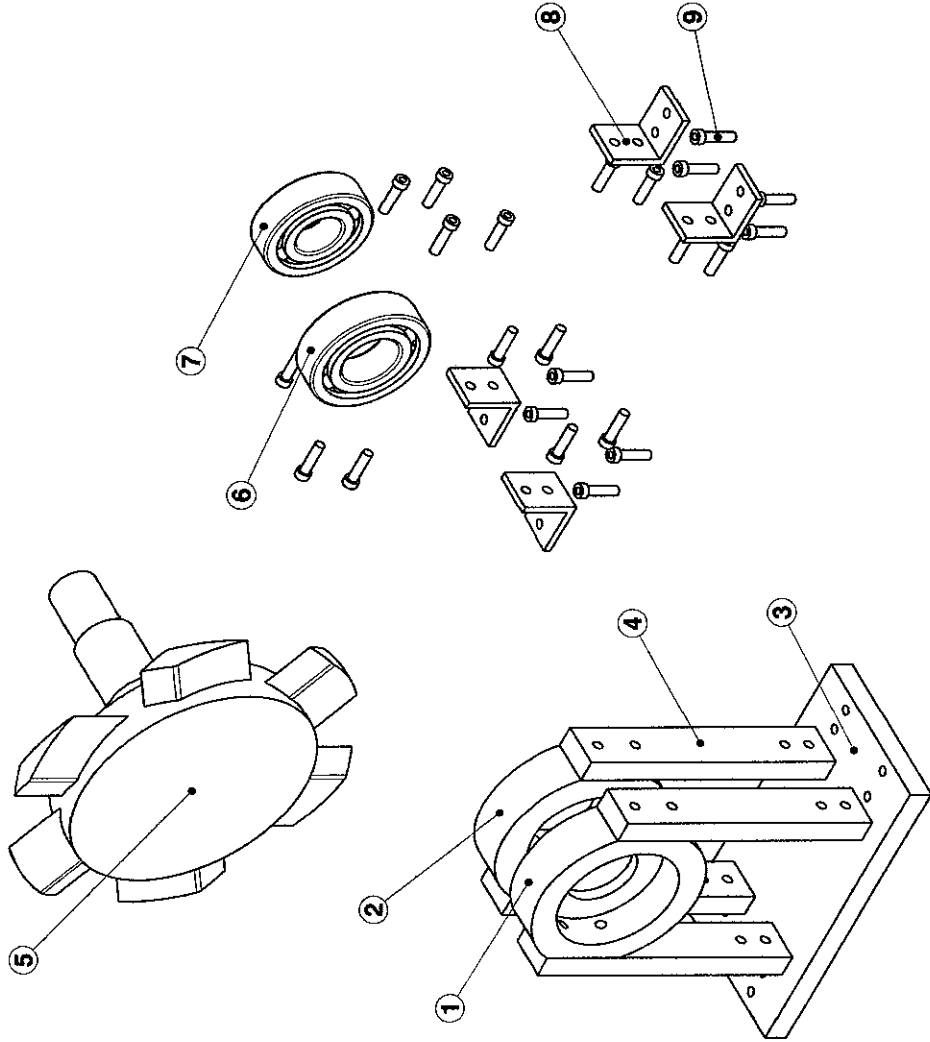
| | | | Fillet Radius, mm | Shoulder Diameter, mm | | Load Rating, kN | |
|----------|--------|-----------|-------------------------|--------------------------|-------|-----------------|-------|
| Bore, mm | OD, mm | Width, mm | | d_s | d_h | Deep Groove | |
| | | | | | | C | C_0 |
| 17 | 40 | 12 | 0.6 | 19.5 | 34 | 9.56 | 4.50 |
| 20 | 47 | 14 | 1.0 | 25 | 41 | 12.7 | 6.20 |
| 25 | 52 | 15 | 1.0 | 30 | 47 | 14.0 | 6.95 |
| 30 | 62 | 16 | 1.0 | 35 | 55 | 19.5 | 10.0 |

Table 3: Dimensions and Load Ratings for Single-Row 02 Series Deep-Groove

APPENDIX II

Drawing for First Prototype Configuration
Drawing for Second Prototype Configuration

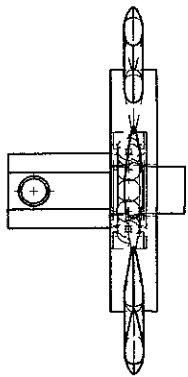
NOTE: 1. LH SHOW RH SYMM OPF.
 2. ALL SHARP CORNER CHAMFER 1mm UNLESS OTHERWISE SHOWN.
 3. ALL JOINING AREA SHALL BE ▽ UNLESS SPECIFIED.



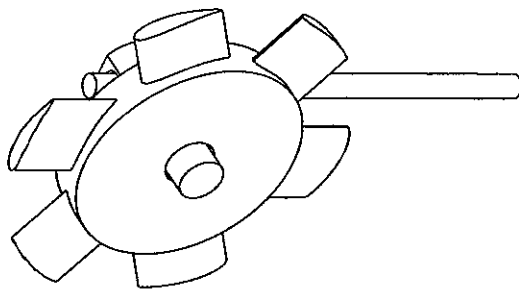
| | | |
|------------------------|-------|-------------|
| ⑤ 24 BOLT | STEEL | M10X1.25 |
| ⑥ 4 L-BRACKET | ALUM | 11X10X10 |
| ⑦ 1 BEARING Ø20 | ALUM | 11X8X7 |
| ⑧ 1 BEARING Ø20 | ALUM | 11X8X7 |
| ⑨ 1 ROTOR & SHAFT TUBE | ALUM | 120X119X160 |
| ⑩ 1 SUPPORT | ALUM | 110X116X20 |
| ⑪ 1 BASE | WOOD | 110X139X75 |
| ⑫ 1 MOUNTING 2 | ALUM | 120X75 |
| ⑬ 1 MOUNTING 1 | ALUM | 120X75 |
| ⑭ 1 MOUNTING 3 | ALUM | 120X75 |
| ⑮ 1 MOUNTING 4 | ALUM | 120X75 |
| ⑯ 1 MOUNTING 5 | ALUM | 120X75 |
| ⑰ 1 MOUNTING 6 | ALUM | 120X75 |
| ⑱ 1 MOUNTING 7 | ALUM | 120X75 |
| ⑲ 1 MOUNTING 8 | ALUM | 120X75 |
| ⑳ 1 MOUNTING 9 | ALUM | 120X75 |
| ⑳ 1 MOUNTING 10 | ALUM | 120X75 |
| ⑳ 1 MOUNTING 11 | ALUM | 120X75 |
| ⑳ 1 MOUNTING 12 | ALUM | 120X75 |
| ⑳ 1 MOUNTING 13 | ALUM | 120X75 |
| ⑳ 1 MOUNTING 14 | ALUM | 120X75 |
| ⑳ 1 MOUNTING 15 | ALUM | 120X75 |
| ⑳ 1 MOUNTING 16 | ALUM | 120X75 |
| ⑳ 1 MOUNTING 17 | ALUM | 120X75 |
| ⑳ 1 MOUNTING 18 | ALUM | 120X75 |
| ⑳ 1 MOUNTING 19 | ALUM | 120X75 |
| ⑳ 1 MOUNTING 20 | ALUM | 120X75 |
| ⑳ 1 MOUNTING 21 | ALUM | 120X75 |
| ⑳ 1 MOUNTING 22 | ALUM | 120X75 |
| ⑳ 1 MOUNTING 23 | ALUM | 120X75 |
| ⑳ 1 MOUNTING 24 | ALUM | 120X75 |
| ⑳ 1 MOUNTING 25 | ALUM | 120X75 |
| ⑳ 1 MOUNTING 26 | ALUM | 120X75 |
| ⑳ 1 MOUNTING 27 | ALUM | 120X75 |
| ⑳ 1 MOUNTING 28 | ALUM | 120X75 |
| ⑳ 1 MOUNTING 29 | ALUM | 120X75 |
| ⑳ 1 MOUNTING 30 | ALUM | 120X75 |
| ⑳ 1 MOUNTING 31 | ALUM | 120X75 |
| ⑳ 1 MOUNTING 32 | ALUM | 120X75 |
| ⑳ 1 MOUNTING 33 | ALUM | 120X75 |
| ⑳ 1 MOUNTING 34 | ALUM | 120X75 |
| ⑳ 1 MOUNTING 35 | ALUM | 120X75 |
| ⑳ 1 MOUNTING 36 | ALUM | 120X75 |
| ⑳ 1 MOUNTING 37 | ALUM | 120X75 |
| ⑳ 1 MOUNTING 38 | ALUM | 120X75 |
| ⑳ 1 MOUNTING 39 | ALUM | 120X75 |
| ⑳ 1 MOUNTING 40 | ALUM | 120X75 |
| ⑳ 1 MOUNTING 41 | ALUM | 120X75 |
| ⑳ 1 MOUNTING 42 | ALUM | 120X75 |
| ⑳ 1 MOUNTING 43 | ALUM | 120X75 |
| ⑳ 1 MOUNTING 44 | ALUM | 120X75 |
| ⑳ 1 MOUNTING 45 | ALUM | 120X75 |
| ⑳ 1 MOUNTING 46 | ALUM | 120X75 |
| ⑳ 1 MOUNTING 47 | ALUM | 120X75 |
| ⑳ 1 MOUNTING 48 | ALUM | 120X75 |
| ⑳ 1 MOUNTING 49 | ALUM | 120X75 |
| ⑳ 1 MOUNTING 50 | ALUM | 120X75 |
| ⑳ 1 MOUNTING 51 | ALUM | 120X75 |
| ⑳ 1 MOUNTING 52 | ALUM | 120X75 |
| ⑳ 1 MOUNTING 53 | ALUM | 120X75 |
| ⑳ 1 MOUNTING 54 | ALUM | 120X75 |
| ⑳ 1 MOUNTING 55 | ALUM | 120X75 |
| ⑳ 1 MOUNTING 56 | ALUM | 120X75 |
| ⑳ 1 MOUNTING 57 | ALUM | 120X75 |
| ⑳ 1 MOUNTING 58 | ALUM | 120X75 |
| ⑳ 1 MOUNTING 59 | ALUM | 120X75 |
| ⑳ 1 MOUNTING 60 | ALUM | 120X75 |
| ⑳ 1 MOUNTING 61 | ALUM | 120X75 |
| ⑳ 1 MOUNTING 62 | ALUM | 120X75 |
| ⑳ 1 MOUNTING 63 | ALUM | 120X75 |
| ⑳ 1 MOUNTING 64 | ALUM | 120X75 |
| ⑳ 1 MOUNTING 65 | ALUM | 120X75 |
| ⑳ 1 MOUNTING 66 | ALUM | 120X75 |
| ⑳ 1 MOUNTING 67 | ALUM | 120X75 |
| ⑳ 1 MOUNTING 68 | ALUM | 120X75 |
| ⑳ 1 MOUNTING 69 | ALUM | 120X75 |
| ⑳ 1 MOUNTING 70 | ALUM | 120X75 |
| ⑳ 1 MOUNTING 71 | ALUM | 120X75 |
| ⑳ 1 MOUNTING 72 | ALUM | 120X75 |
| ⑳ 1 MOUNTING 73 | ALUM | 120X75 |
| ⑳ 1 MOUNTING 74 | ALUM | 120X75 |
| ⑳ 1 MOUNTING 75 | ALUM | 120X75 |
| ⑳ 1 MOUNTING 76 | ALUM | 120X75 |
| ⑳ 1 MOUNTING 77 | ALUM | 120X75 |
| ⑳ 1 MOUNTING 78 | ALUM | 120X75 |
| ⑳ 1 MOUNTING 79 | ALUM | 120X75 |
| ⑳ 1 MOUNTING 80 | ALUM | 120X75 |
| ⑳ 1 MOUNTING 81 | ALUM | 120X75 |
| ⑳ 1 MOUNTING 82 | ALUM | 120X75 |
| ⑳ 1 MOUNTING 83 | ALUM | 120X75 |
| ⑳ 1 MOUNTING 84 | ALUM | 120X75 |
| ⑳ 1 MOUNTING 85 | ALUM | 120X75 |
| ⑳ 1 MOUNTING 86 | ALUM | 120X75 |
| ⑳ 1 MOUNTING 87 | ALUM | 120X75 |
| ⑳ 1 MOUNTING 88 | ALUM | 120X75 |
| ⑳ 1 MOUNTING 89 | ALUM | 120X75 |
| ⑳ 1 MOUNTING 90 | ALUM | 120X75 |
| ⑳ 1 MOUNTING 91 | ALUM | 120X75 |
| ⑳ 1 MOUNTING 92 | ALUM | 120X75 |
| ⑳ 1 MOUNTING 93 | ALUM | 120X75 |
| ⑳ 1 MOUNTING 94 | ALUM | 120X75 |
| ⑳ 1 MOUNTING 95 | ALUM | 120X75 |
| ⑳ 1 MOUNTING 96 | ALUM | 120X75 |
| ⑳ 1 MOUNTING 97 | ALUM | 120X75 |
| ⑳ 1 MOUNTING 98 | ALUM | 120X75 |
| ⑳ 1 MOUNTING 99 | ALUM | 120X75 |
| ⑳ 1 MOUNTING 100 | ALUM | 120X75 |

APPROVED BY: _____ DRAWN BY: MESAT FAZLI
 CHECKED BY: DR. AZMI MATERIAL: ALUMINIUM
 SCALE: 1:1
 SURF FINISH: ▽
 HEAT TREATMENT: ▽
 DIMENSIONS: UNLESS SPECIFIED
 SURF: UNLESS SPECIFIED
 CORE: UNLESS SPECIFIED
 U.P.C. NO.: SAFETY PARTING CLASSIFICATION: ASSEMBLY DRAWING
 DRAWING NAME: 1ST CONFIGURATION-WELLS TURBINE PROTOTYPE
 DRAWING NO.: DRPTWT-00017 (7/7)
 STATE: RELEASE
 CONFIDENTIAL

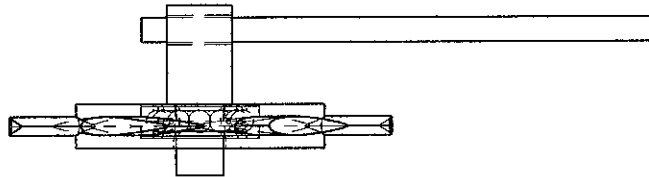
- NOTE; 1. LH SHOWN RH SYMM LPP.
 2. ALL SHARP CORNER CHAMFER 1mm UNLESS OTHERWISE SHOWN.
 3. ALL JOINING AREA SHALL BE VV UNLESS SPECIFIED.



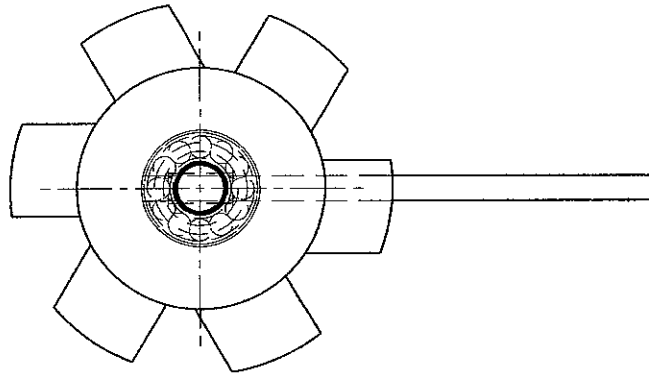
Top view
Scale: 1:1



Isometric view
Scale: 1:1



Right view
Scale: 1:1

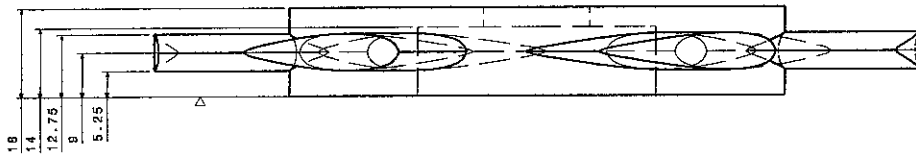


Front view
Scale: 1:1

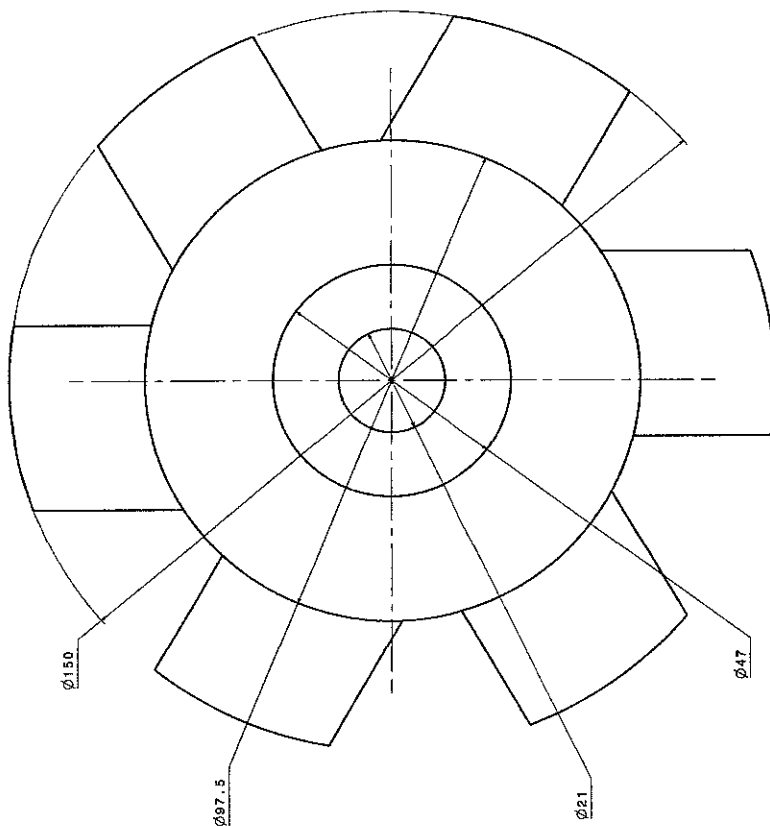
| | | | | | | | | | |
|-------------------------------|--|-------------------------|--|--------------------------|--|---|--|------------------------------------|--|
| 100% ± ITL -100% ± H/L | | APPROVED BY DR. AZMI | | CHECKED BY DR. AZMI | | DRAWN BY MEGAT FAZLI | | DATE 24/04/09 | |
| THIRD ANGLE PROJECTION | | SCALE NTS | | MATERIAL TJ88 & STEEL | | TOLEANCE UNLESS SPECIFIED ±0.5 | | REFERENCE BASE | |
| FURNISHING 1. HARD COPR | | SURF ROUGNESS | | SAFETY PART | | TOLERANCE UNLESS SPECIFIED ±0.5 | | REFERENCE BASE | |
| TITLES 1. REV. 1 | | VERT TREATMENT | | UPC NO. | | PLANNING DRAWING | | STATE RELEAS | |
| TOTAL EFFECTIVE CASE DEPTH | | SAFETY PART | | DRAWING NAME | | 2ND CONFIGURATION-WELLS TURBINE PROTOTYPE | | DRAWING NO. DRPTWT-00021 (1/15) | |
| HARD COPR | | SAFETY PART | | DRAWING NAME | | 2ND CONFIGURATION-WELLS TURBINE PROTOTYPE | | DRAWING NO. DRPTWT-00021 (1/15) | |
| HARD COPR | | SAFETY PART | | DRAWING NAME | | 2ND CONFIGURATION-WELLS TURBINE PROTOTYPE | | DRAWING NO. DRPTWT-00021 (1/15) | |
| HARD COPR | | SAFETY PART | | DRAWING NAME | | 2ND CONFIGURATION-WELLS TURBINE PROTOTYPE | | DRAWING NO. DRPTWT-00021 (1/15) | |
| HARD COPR | | SAFETY PART | | DRAWING NAME | | 2ND CONFIGURATION-WELLS TURBINE PROTOTYPE | | DRAWING NO. DRPTWT-00021 (1/15) | |
| HARD COPR | | SAFETY PART | | DRAWING NAME | | 2ND CONFIGURATION-WELLS TURBINE PROTOTYPE | | DRAWING NO. DRPTWT-00021 (1/15) | |

CONFIDENTIAL

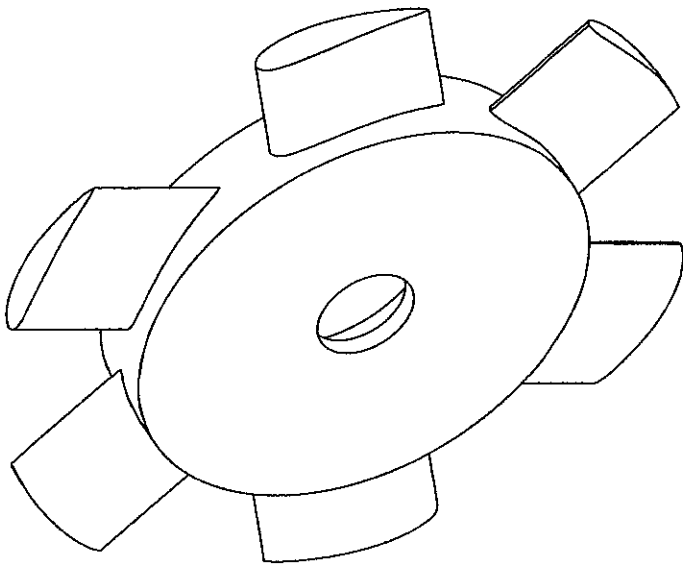
- NOTE: 1. ALL SHARP CORNER CHAMFER 1mm UNLESS OTHERWISE SHOWN.
- 2. ALL SHARP CORNER CHAMFER 1mm UNLESS OTHERWISE SHOWN.
- 3. ALL JOINING AREA SHALL BE VV UNLESS SPECIFIED.



Right view
Scale: 2:1



Front view
Scale: 2:1

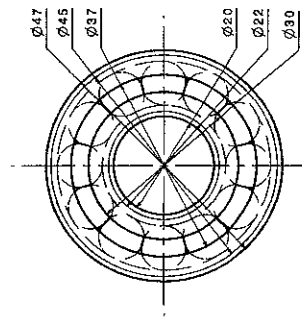


Isometric view
Scale: 2:1

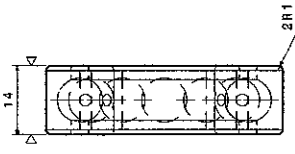
| | | | | | |
|----------------------------|-----|--------------------|----------|--------------------------------|---|
| 1 ROTOR | | TJ988 | TJ6X150 | REVISIONS | |
| SYMBOL / JIG LOCATOR NAME | | MATERIAL CLASS | | SUBMIT DATE | |
| APPROVED BY | | DR. AZMI | DR. AZMI | MEGAT FAZLI | 24/04/09 |
| SCALE | NTS | PHOS | Kg | MATERIAL | TJ688 |
| SURF. FINISH | VV | VV | VV | TOLERANCE UNLESS SPECIFIED | REFERENCE BASE |
| HEAT TREATMENT | | | | UNLESS SPECIFIED | 30.5 |
| TOTAL EFFECTIVE USE PERIOD | | | | SAFETY PART D/C CLASSIFICATION | FABRICATION DRAWING |
| PRODUCTION | | | | DRAWING NAME | 2ND CONFIGURATION-WELLS TURBINE PROTOTYPE |
| PRODUCTION | | | | DESIGNED WITH DATA VERSIONAL 2 | UNIVERSITY Technology of PERANG |
| CONFIDENTIAL | | DRAWING NO. | | STATE | |
| | | DPRWT-00022 (2/15) | | RELEASE | |

1 ROTOR

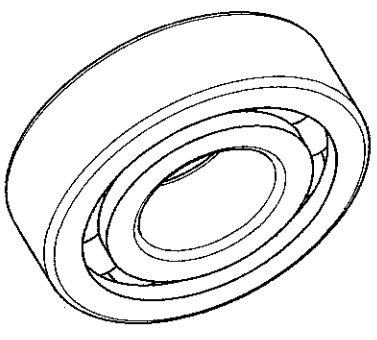
NOTE: 1. LH. SHOWN RH. SYMM. OPP.
 2. ALL SHARP CORNER CHAMFER .1mm UNLESS OTHERWISE SHOWN.
 3. ALL JOINING AREA SHALL BE VV UNLESS SPECIFIED.



Front View
Scale: 2:1



Right View
Scale: 2:1



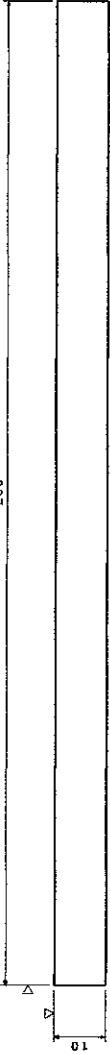
Isometric view
Scale: 3:1

2 GROOVE BALL BEARING Ø20

| | | | | | | | | | |
|--------------|--|--------|--|-------------------------|--|------------------------------------|--|-------------------------------------|--|
| 100X - 1TL | | FINISH | | APPROVED BY | | MATERIAL CLASS | | REMARKS | |
| - 100Y - 1BL | | X | | DR. AZBI | | DR. AZBI | | SUPPLY DATE | |
| 100Z - 1AL | | X | | SCALE: MTS | | MATERIAL | | 24/04/09 | |
| VIEW: X(1) | | X(1) | | SURF. FINISHES | | Kg | | STEEL | |
| X(2) | | X(2) | | HEAT TREATMENT | | TOLERANCE UNLESS SPECIFIED | | REFERENCE BASE | |
| X(3) | | X(3) | | TOTAL SPECIFIC USE ONLY | | UPC NO. | | FABRICATION DRAWING | |
| X(4) | | X(4) | | CORE | | SAFETY PART (DG CLASSIFICATION) | | 2ND CONFIGURATION-TURBINE PROTOTYPE | |
| X(5) | | X(5) | | X(5) | | DRAWING NAME | | DRAWING NO. | |
| X(6) | | X(6) | | X(6) | | UNIVERSITY TECHNOLOGY OF PETROBRAS | | DRAWING NO. DRPTWT-00023 (3/5) | |
| X(7) | | X(7) | | X(7) | | STATE | | RELEASE | |
| X(8) | | X(8) | | X(8) | | STATE | | RELEASE | |

CONFIDENTIAL

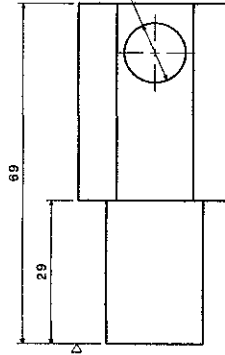
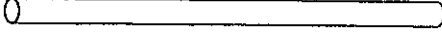
NOTE: 1. LH SHOWN RH SYMM OPP.
 2. ALL SHARP CORNER CHAMFER 1mm UNLESS OTHERWISE SHOWN.
 3. ALL JOINING AREA SHALL BE VV UNLESS SPECIFIED.



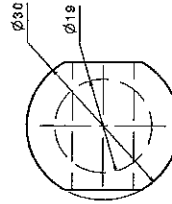
Front view
Scale: 2:1

3 ROD

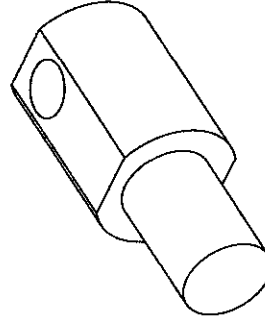
Isometric view
Scale: 1:1



Front view
Scale: 2:1



Right view
Scale: 2:1

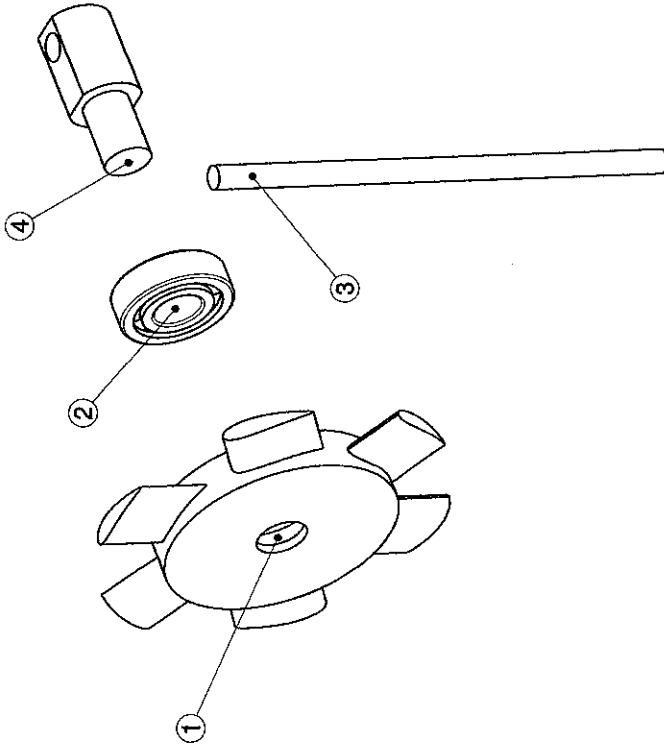


Isometric view
Scale: 2:1

| | | | | | | | | | |
|------------------------|-----------|----------------------------|----------|-----------------------------------|--------------------|---|-------------|-------------|----------|
| FINISH | 100% - TL | APPROVED BY | DR. AZMI | CHECKED BY | DR. AZMI | DRAWN BY | MEGAT FAZLI | SUBMIT DATE | 24/04/09 |
| 100% - BL | | SCALE | MSS | MATERIAL | TJ88 & STEEL | REFERENCE BAGE | | | |
| 100% - FL | | HEAT TREATMENT | ROD-PHOS | SAFETY PART | DWG CLASSIFICATION | 2ND CONFIGURATION-WELLS TURBINE PROTOTYPE | | | |
| THIRD ANGLE PROJECTION | | TOTAL EFFECTIVE CASE DEPTH | | UPC NO. | | | | | |
| FULL CROSS SECTION | | ROD-PHOS | | DRAWING NAME | | FABRICATION DRAWING | | | |
| XI ENCLOSURE | | ROD-PHOS | | UNIVERSITY TECHNOLOGY of PETRONAS | | | | | |
| XI HARD COPY | | | | DRAWING NO. | | DRPTWT-00024 (4/5) | | | |
| | | | | STATE | | | | | |
| | | | | RELEASE | | | | | |

4 SHAFT

- NOTE: 1. LH SHOWN RH SYMM OPP.
 2. ALL SHARP CORNER CHAMFER 1mm UNLESS OTHERWISE SHOWN.
 3. ALL JOINING AREA SHALL BE ∇ UNLESS SPECIFIED.



Isometric view
Scale: 1:1

| | | | | | | | | | |
|-------------|--|--------|--|------------------------------------|--|---|--|--------------------|--|
| 100% I TL | | FINISH | | APPROVED BY | | DRAWN BY | | SUBMIT DATE | |
| -100% I BEL | | | | DR. AZMI | | MEGAT FAZLI | | 24/04/09 | |
| 100% I VAL | | | | MNS | | MATERIAL | | TUBE & STEEL | |
| 100% I TBL | | | | NTS | | KG | | | |
| 100% I TBL | | | | SURF | | TOLERANCE | | REFERENCE BASE | |
| 100% I TBL | | | | ROUNDS | | UNLESS SPECIFIED | | ±0.5 | |
| 100% I TBL | | | | UFC NO. | | SAFETY PART ING CLASSIFICATION | | ASSEMBLY DRAWING | |
| 100% I TBL | | | | DRAWING NAME | | 2ND CONFIGURATION-WELLS TURBINE PROTOTYPE | | | |
| 100% I TBL | | | | UNIVERSITY Technology of PETROSUIS | | DRAWING NO. | | DRPTMT-00225 (S/S) | |
| 100% I TBL | | | | CONFIDENTIAL | | | | STATE RELEASE | |